We are IntechOpen, the world's leading publisher of Open Access books Built by scientists, for scientists

6,900
Open access books available

185,000
International authors and editors

200M
Downloads

Our authors are among the

154
Countries delivered to

TOP 1%
most cited scientists

12.2%
Contributors from top 500 universities

WEB OF SCIENCE™

Selection of our books indexed in the Book Citation Index in Web of Science™ Core Collection (BKCI)

Interested in publishing with us?
Contact book.department@intechopen.com

Numbers displayed above are based on latest data collected.
For more information visit www.intechopen.com

16

Fourier Transforms Infrared Spectroscopy Applied in Selective Catalytic Reduction of NO by Acetylene

Xinping Wang
Dalian University of Technology
China

1. Introduction

Selective catalytic reduction of NO by hydrocarbons (HC-SCR) is believed to be one of the most promising ways to remove nitric oxide from the exhaust gas of diesel and lean-burn engines. Since HC-SCR was reported individually by Iwamoto and Held groups (Iwamoto et al., 1999; Held et al., 1990), many studies were carried out in this field both on new catalyst research and on reaction mechanism. In these studies, Fourier Transforms Infrared Spectroscopy (FTIR) was extensively used for interpreting the relationship between surface structure and the catalytic performance of the catalysts, especially, for disclosing the reaction mechanism over the catalysts. In this chapter, we summarize the FTIR studies used in the investigation of selective catalytic reduction of NO by acetylene (C_2H_2-SCR).

2. To characterize surface acidity of the catalyst

For HC-SCR, many zeolites have been investigated as catalysts. However, it seems that only limited types of zeolites including ZSM-5 (Li et al., 2004; Li et al., 2008; Wang et al., 2007a; Wang et al., 2007b; Wang et al., 2005; Niu et al., 2006), ferrierite (Seijger et al., 2003; Lee et al., 2003; Kubacka et al., 2005; Kubacka et al., 2006) and mordenite (Pieterse & Booneveld, 2007; Mosqueda-Jiménez et al., 2003a; Córdoba et al., 2005; Lónyi et al., 2007; Dorado et al., 2005), which are called as pentasil zeolites, displayed high selectivity to NO_x reduction in HC-SCR. For instance, Pieterse et al. (Pieterse et al., 2003) investigated the selective catalytic reduction of NO by methane (CH_4-SCR) over several zeolite-based catalysts and reported an activity order of Co-Pd-ZSM-5 > Co-Pd-MOR > Co-Pd-FER > Co-Pd-BEA. Abreu and his co-workers (Torre-Abreu et al., 1999) found that zeolites modified by Cu used for selective catalytic reduction of NO by propene (C_3H_8-SCR) are ordered in NO conversion at 400 ^oC with CuMFI (58%) > CuMOR (43%) > CuY (20%). Sultana et al. (Sultana et al., 2008) reported that zeolites are ordered with Pt-MOR (90%) > Pt-FER (77%) > Pt-ZSM-5 (74%) > Pt-BEA (70%) > Pt-HY (63%) in terms of NO conversion for selective catalytic reduction of NO at ~300 ^oC using diesel as reductant. Shibata et al. (Shibata et al., 2004) reported an order of Ag-MFI (56%) > Ag-BEA (38%) > Ag-MOR (11%) >> Ag-Y (2%) in NO conversion at ~300 ^oC for the C_3H_8-SCR assisted by H_2. It was also reported that Co-ZSM-5 (Ivanova et al., 2001) and Ni-ZSM-5 (Mihaylov et al., 2004) are more active than the corresponding Y zeolite promoted by

Co or Ni for the CH_4-SCR. All these results indicated that Y is inferior to the pentasil zeolites for the HC-SCR.

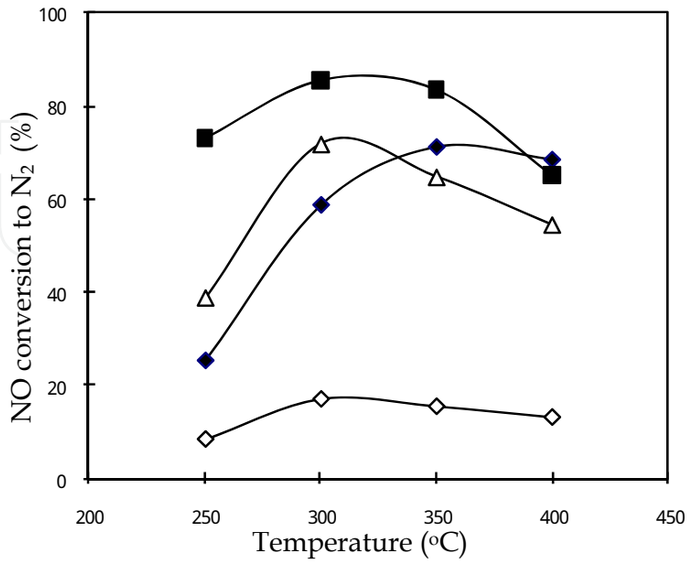

Fig. 1. Conversion of NO_x as a function of temperature over HZSM-5 (◆), HFER (■), HMOR (△) and HY (◇). Reaction conditions: 1600 ppm NO + 800 ppm C_2H_2 + 9.95% O_2 in He with a total flow rate of 50 ml/min over 0.2 g of catalyst

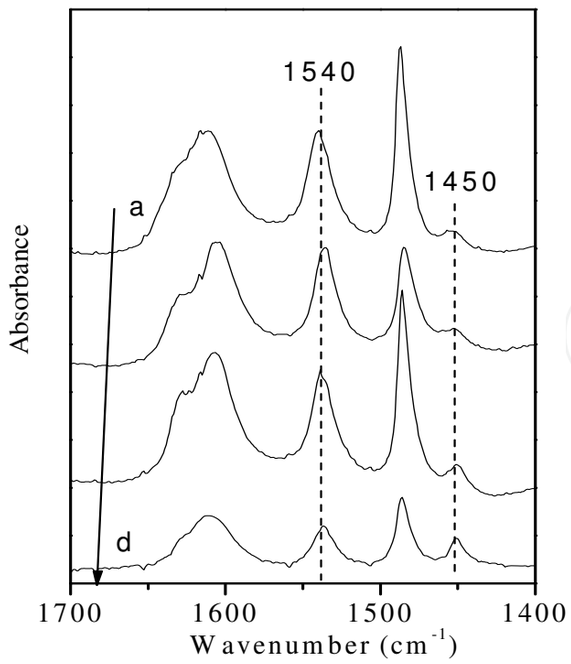

Fig. 2. FTIR spectra of pyridine adsorbed on HZSM-5 (a), HFER (b), HMOR (c) and HY (d) at 500 °C in evacuation

On the other hand, Shichi and co-workers (Shichi et al., 1998; Shichi et al., 2000; Shichi et al., 2001a; Shichi et al., 2001b; Shichi et al., 2004) have emphasized intracrystalline diffusion of reductants limited by the zeolites' channels, based on their investigation results. They found that NO conversion over MFI and MOR appeared to be significantly influenced by both hydrocarbon molecular size and zeolite particle size in some instances. In our investigation of HC-SCR using acetylene as reductant (C_2H_2-SCR), we found that the C_2H_2-SCR over HZSM-5 is greatly affected by the intracrystalline diffusion of NO_2 as well (Wang et al., 2007c). Thus, we suppose that the limited diffusion of the reactants in narrow channels of the pentasil zeolites is the main reason leading to the low NO conversion at high GHSV in HC-SCR. Due to wider channels compared to the pentasil zeolites (Elzey et al., 2008), Y zeolite may be favorable for intracrystalline diffusion of reactants. Besides of this, Y zeolite is stable in severe hydrothermal conditions and economical (Furusawa et al., 2002). Therefore, the zeolite could be expected to be a candidate for preparing a practical catalyst for HC-SCR working at high GHSV, if Y can be effectively modified, due to its larger pore size (0.74 nm × 0.74 nm) than HZSM-5 (0.53 nm × 0.56 nm), HFER(0.42 nm × 0.54 nm) and HMOR (0.65 nm × 0.70). It lead us to study the zeolite in C_2H_2-SCR investigation. However, a result in contrast with the expectation was obtained in the C_2H_2-SCR. HY displayed much low activity compared to HZSM-5, HFER, and HMOR, as shown in Fig 1. To answer the question why HY with the ideal larger pore size exhibited much inferior catalytic performance to the pentasil zeolites in the HC-SCR, we studied the surface acidity of HY in comparison with the pentasil zeolites (Ma et al., 2009). Fig.2 shows FTIR of pyridine adsorbed on different zeolites, obtained by pyridine adsorption over the zeolites and a degassing at 500 ^oC. Compared to HZSM-5, HFER and HMOR, HY gave considerable weaker IR band at 1540 cm^{-1} being associated with pyridine adsorption on protons, indicating that strong Brönsted acids over HY are much less than those of the pentasil zeolites in amount. In literature, zeolites with Na or H form were usually used in HC-SCR investigation as catalyst or support, and opposite results were obtained by the authors on the acidity or basicity of the zeolites favorable for HC-SCR activity, for different HC-SCR catalytic systems. For instance, it was reported that Ag-NaZSM-5 catalyst was more active than Ag-HZSM-5 for the selective catalytic reduction of NO by methane (CH_4-SCR) at 450 °C (Shi et al., 2002), and that Fe-ZSM-5 catalyst with precursor of NaZSM-5 was far more active than that with precursor of NH_4-ZSM-5 for selective catalytic reduction of NO by urea (Sullivan & Keane, 2005). Similarly, high activity for the selective catalytic reduction of NO by propene (C_3H_6-SCR) on Ce-NaZSM-5 (Niu et al., 2006; Seijger et al., 2003) and for CH_4-SCR on Pt-CoNaFER washcoated cordierite monolith (Lee et al., 2003) was obtained. Whereas, Brönsted acids have been suggested by the other authors to be essential for HC-SCR over many catalytic systems (e.g. ZSM-5 modified by Pd, Ga, In, Ce and Ag) (Shibata et al., 2004; Loughran & Resasco, 1995; Kikuchi & Yogo, 1994; Nishizaka & Misono, 1994; Li & Armor, 1994; Narbeshuber et al., 1997; Berndt et al., 2003; Gutierrez et al., 2005).

The authors found that Brönsted acids contributed to the aimed reaction in different steps. For instance, Stakheev and coworkers reported that exchange of partial protons by sodium with a level of 32% resulted in a nearly complete disappearance of the activity of the zeolite for oxidation of NO to NO_2, and a significant decrease of the activity for C_3H_6-SCR (Gutierrez et al., 2005). In the C_2H_2-SCR, we found that the proton form of ZSM-5 based catalyst were much active, whereas the sodium form of ZSM-5 based catalyst almost inactive for the reaction (Wang et al., 2007a; Wang et al., 2005), as shown in table 1. We also found that, with SiO_2/Al_2O_3 ratio of HZSM-5 increasing, C_2H_2-SCR activity of the

HZSM-5 based catalysts (e.g. Ce-HZSM-5, 2%Mo/HZSM-5 and 2%Zr/HZSM-5(Wang et al. 2008) as shown in table 2) decreased in same reaction conditions. These results indicated that protons presenting in the zeolites is indispensable for C_2H_2-SCR and activity of the catalyst strongly depends on the population of protons in the zeolites. Thus, one could believe that it is the weaker surface acidity of HY compared to those of pentasil zeolites which leads to the inferior catalytic performance of HY in comparison with HZSM-5, HFER and HMOR.

Catalysts	Reaction temperature (°C)	NO conv. to N_2 (100%)	Total C_2H_2 conv. (100%)
HZSM-5	300	58.9	86.6
NaZSM-5	325	~0	8.0
Ce-HZSM-5	300	83.0	98.9
Ce-NaZSM-5	300	~0	15.3
Mo-HZSM-5	350	82.7	100
Mo-NaZSM-5	350	~0	14.7

Table 1. Catalytic performance of Na-, and HZSM-5 based catalysts in C_2H_2-SCR*
*Note: All of the catalyst were prepared from ZSM-5 with SiO_2/Al_2O_3 of 25

Reaction conditions: 1600 ppm NO + 800 ppm C_2H_2 + 9.95% O_2 in He with a total flow rate of 50 ml/min over 0.2 g of catalyst.

Catalyst with SiO_2/Al_2O_3 ratio	Reaction temperature (°C)	NO conv. to N_2 (100%)	Total C_2H_2 conv. (100%)
Ce-25	300	83.0	98.9
Ce-38	300	64.2	100
Ce-50	300	~0	79
Mo-25	350	82.7	100
Mo-38	350	57.7	100
Mo-50	350	48.0	100
Zr-25	350	89	100
Zr-38	350	73	100
Zr-50	350	66	100

Table 2. Catalytic performance of Ce-HZSM-5, 2%Mo/HZSM-5 and 2%Zr/HZSM-5 prepared from the zeolite with different SiO_2/Al_2O_3 ratio*
*Note: Ce-HZSM-5 was prepared by ion exchange, and 2%Mo/HZSM-5 and 2%Zr/HZSM-5 were prepared by impregnation

3. To confirm rate-determining step

Over many kinds of catalysts, HC-SCR was believed to be initiated from NO oxidation to NO_2, and the step was generally accepted to be crucial step (Kubacka et al., 2006; Pieterse & Booneveld, 2007). To elucidate why HY displayed inferior catalytic performance in C_2H_2-SCR, activity of HY for NO oxidation to NO_2 was compared to those of HZSM-5, HFER and HMOR. As shown in Fig. 3, all of the pentasil zeolites exhibited considerably higher activity compared to HY, in particular, in the case of HFER at 250 °C. The results implies that the reaction of $NO + O_2 \longrightarrow NO_2$ is catalyzed by acid sites of the zeolite. It was strongly supported by experimental results that when sodium form of ZSM-5 was used as catalyst for the reaction of NO oxidation, almost no catalytic activity could be observed. Combined the catalytic activity of the zeolites both for NO oxidation and for C_2H_2-SCR of NO, it can be found that the curves of NO oxidation to NO_2
vs. reaction temperature resemble much to those of NO conversion to N_2 in C_2H_2-SCR in patterns, indicating that C_2H_2-SCR is significantly confined by the step of $NO + O_2 \longrightarrow NO_2$ over HY.

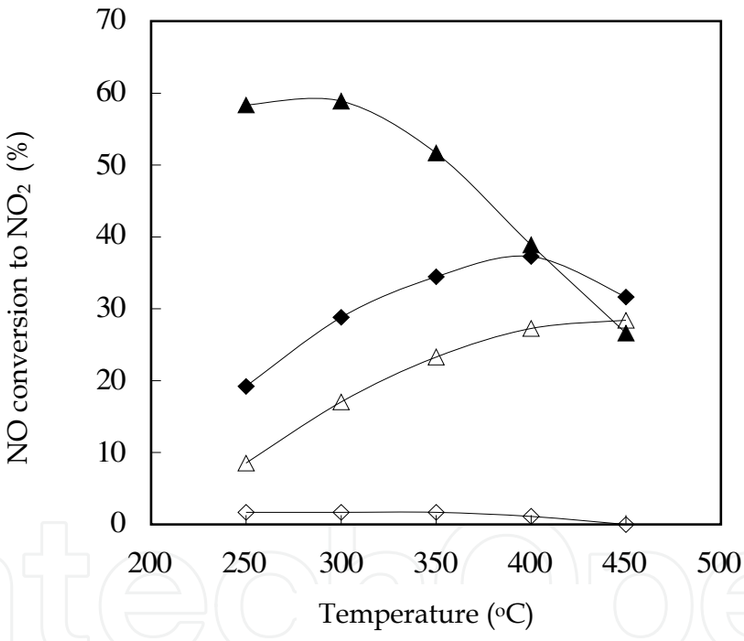

Fig. 3. Catalytic performance of HZSM-5 (◆), HFER (▲), HMOR (△) and HY (◇) in oxidation of NO with O_2 at different temperatures. Reaction conditions: 200 ppm NO + 10% O_2 in N_2 was fed to 0.200 g at a total flow rate of 100 ml/min

For C_2H_2-SCR over HZSM-5 and HFER, it can be speculated that the step of NO oxidation to NO_2 may not be the rate-determining step, as the two zeolites are rather active to NO oxidation, due to their lager amount of protons characterized by FTIR of pyridine adsorption (Fig. 2). The speculation was confirmed by the following experimental results. As shown in Fig. 4, although HZSM-5 itself is more active for NO oxidation with O_2 at the reaction temperature ranged from 200~400 °C than all of xY/HZSM-5 (x = 0 ~ 9), it gave a rather lower NO conversion to N_2 compared to 3%Y/HZSM-5, as shown in Fig. 5 (Wang et

al., 2008). To investigate the rate-determining step of C_2H_2-SCR over these catalysts, and effectively research more active catalyst for the reaction of C_2H_2-SCR, several possible step for the reaction over the catalysts, such as NO_x adsorption over the catalysts and the activity of the nitrous species toward reduction over the catalysts were investigated. At first, FTIR spectrum arising from nitrous species on HZSM-5 and 3%Y/HZSM-5 after saturated co-adsorption of $NO+O_2$ was measured at 250 °C, as shown in Fig. 6. Compared to HZSM-5, 3%Y/HZSM-5 gave significantly stronger band at 1585 cm^{-1} due to bidentate nitrates (Ivanova et al., 2001; Yu et al., 2004; Shimizu et al., 2001; He et al., 2004; Poignant et al., 2001) and a new band at 1609 cm^{-1} caused by $NO+O_2$ saturated co-adsorption at 250 °C. The results indicated that the nitrous species adsorption capacity of 3%Y/HZSM-5 is much stronger in comparison with that of HZSM-5. NO- and NO_2-TPD on the catalyst samples gave also the same conclusion. As shown in Fig. 7, substantially larger amounts of NO and NO_2 were measured in the temperature range of 250-550 °C on 3%Y/HZSM-5 in the NO_x-TPD compared to that on HZSM-5. It should be noted that the corresponding nitrous species which desorbed from the catalyst surface in the temperature range quite seems to be those reacting with C_2H_2 and contributing C_2H_2-SCR of NO, as large parts of them could be speculated to stay on the catalyst surface at the C_2H_2-SCR reaction conditions. By combining the C_2H_2-SCR activity with the nitrous species adsorption capacity of the catalysts, a consistent relationship was obtained for Mo-(Wang et al., 2007a), W-(Wang et al., 2007b), Zr-promoted HZSM-5 as well as Zr-promoted HFER, i.e. by these metals incorporating into HZSM-5 and HFER, nitrous species adsorption capacity of the catalyst was significantly enhanced, and at the same time, C_2H_2-SCR activity of the catalyst was largely improved.

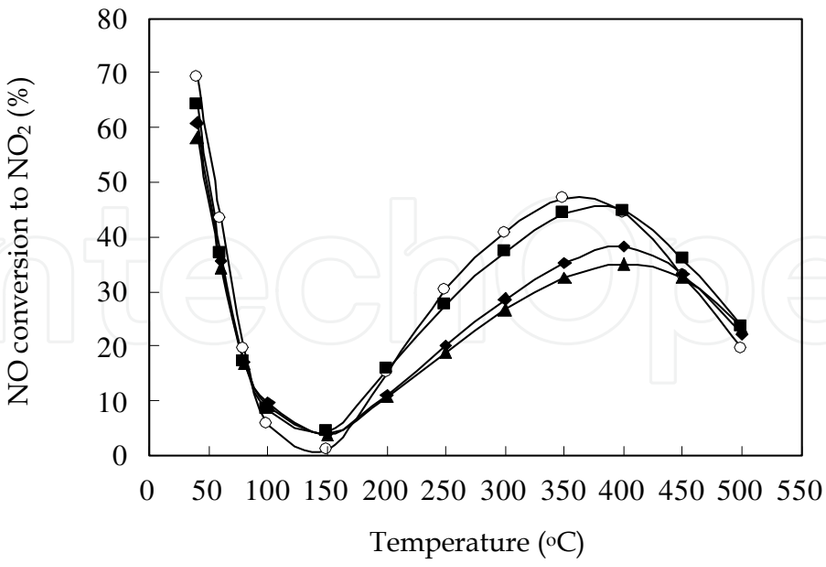

Fig. 4. Catalytic activity of xY/HZSM-5 for NO oxidation with O_2: x=0 (○), x=0.5 (■), x=3 (♦) and x=9 (▲). Reaction conditions: 200 ppm NO, 10 % O_2 in N_2 with a total flow rate of 100 ml/min over 0.200 g catalysts

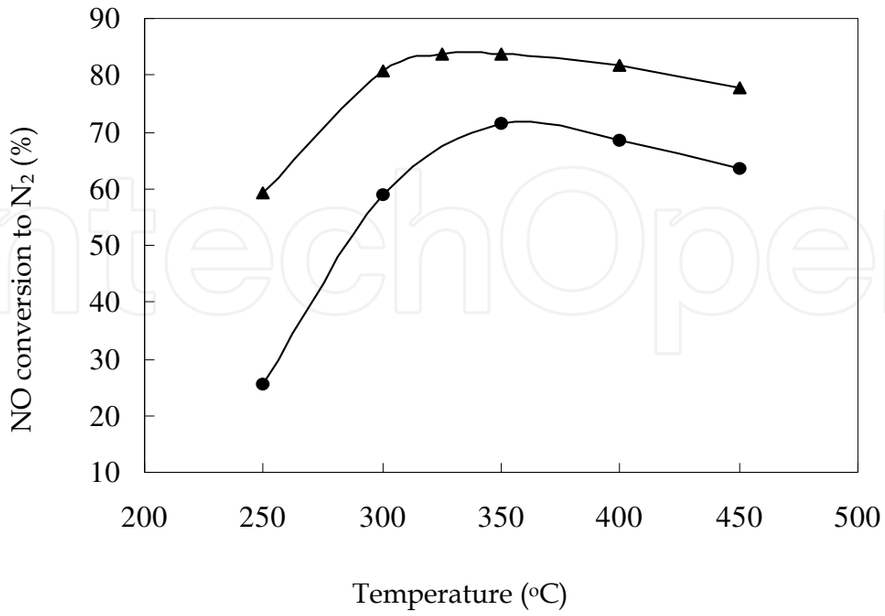

Fig. 5. NO conversion to N_2 as a function of reaction temperature over HZSM-5 (●), and 3%Y/HZSM-5 (▲). Reaction condition: 1600 ppm NO, 800 ppm C_2H_2, 9.95% O_2 in He with a total flow rate of 50 ml·min^{-1} over 0.200 g of catalyst

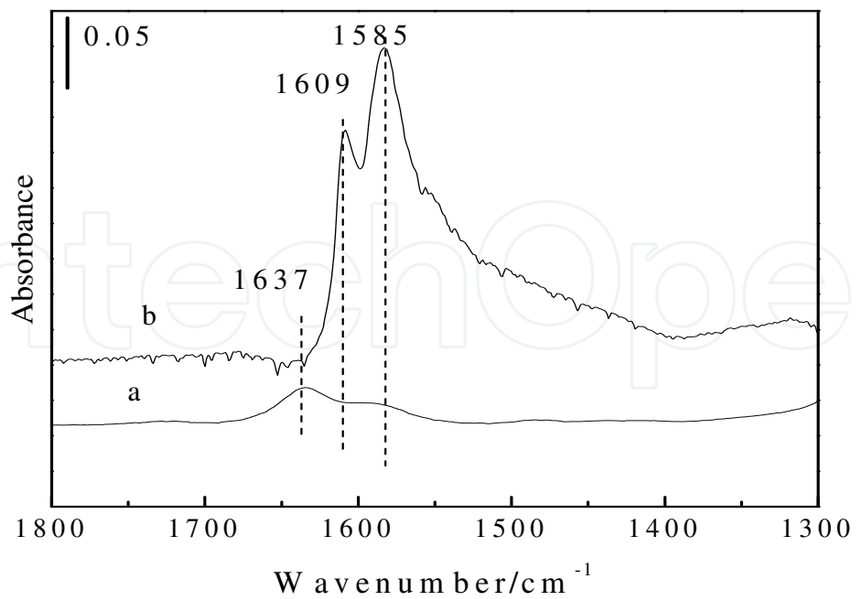

Fig. 6. FTIR spectra arising from nitrous species on HZSM-5 (a) and 3% Y/HZSM-5 (b) after saturated co-adsorption of NO+O_2 at 250 °C

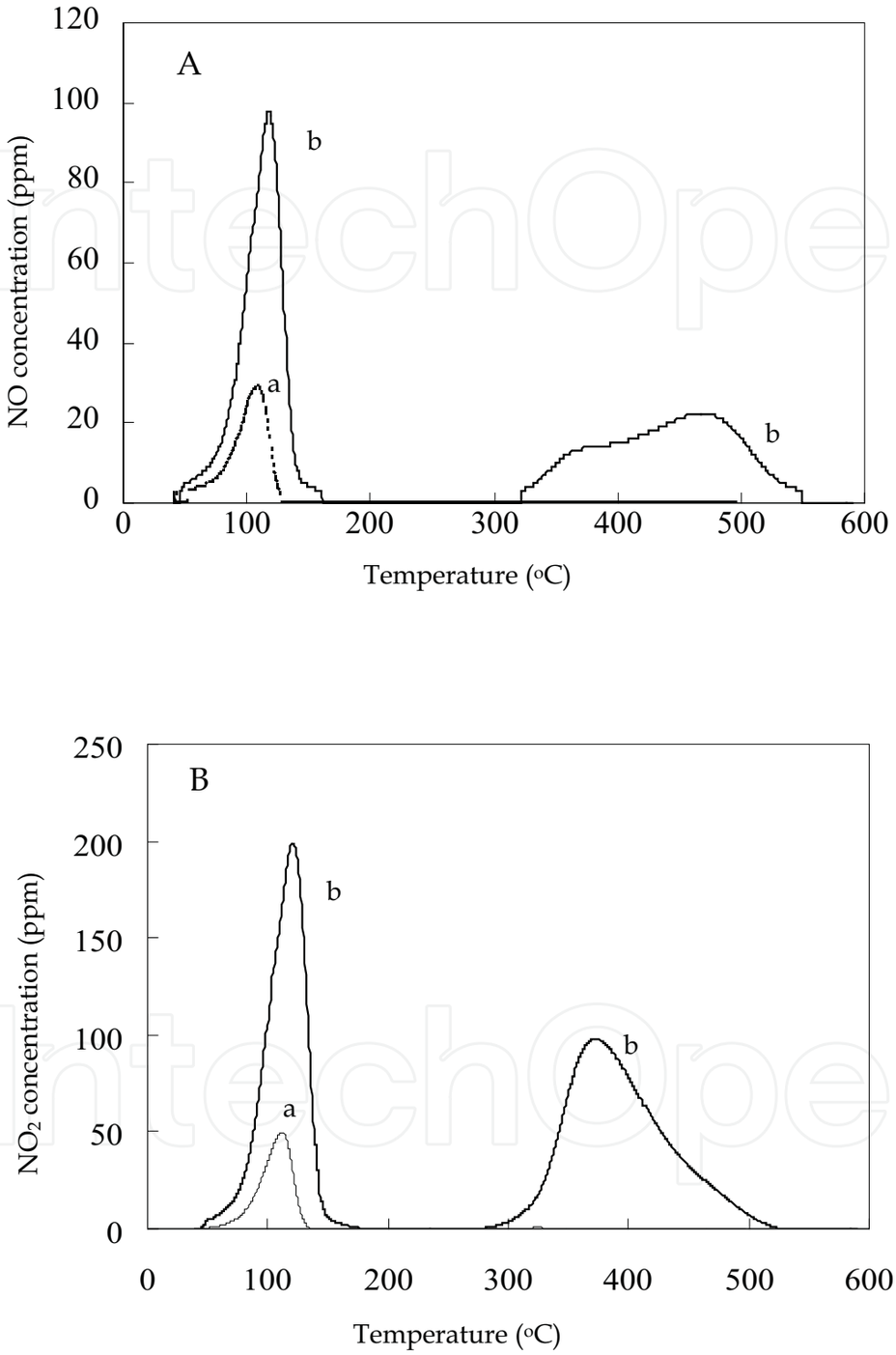

Fig. 7. TPD profiles of NO (A) and NO_2 (B) over HZSM-5 (a) and 3% Y/HZSM-5 (b) after saturated co-adsorption of $NO+O_2$

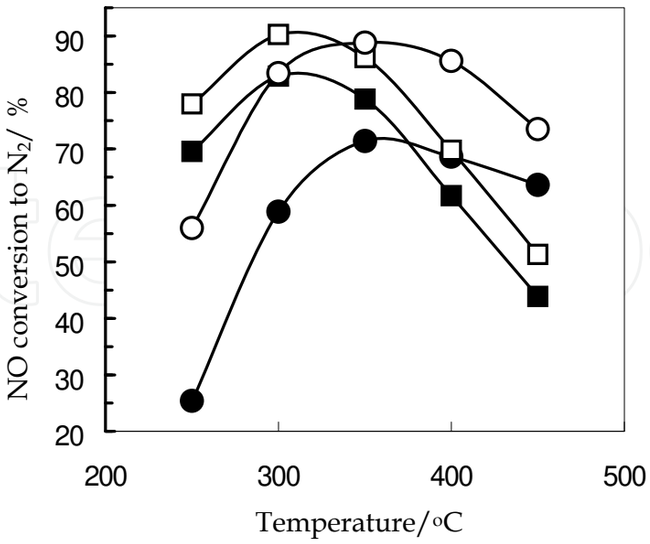

Fig. 8. The NO conversion to N_2 as a function of temperature over HZSM-5 (●), 2%Zr/HZSM-5 (○), HFER (■) and 2%Zr/HFER (□). The reaction conditions are the same as that in Fig. 5

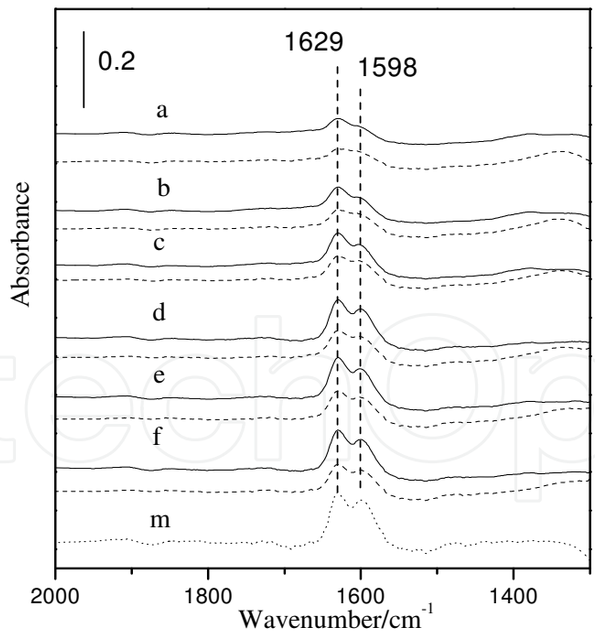

Fig. 9. Transient FTIR spectra at 250 ◦C upon HFER (solid curve) and HZSM5 (dashed curve) exposing to 1000 ppm NO + 10 % O_2 in N_2 (A) for 1 min (a), 2 min (b), 5 min (c), 10 min (d), 15 min (e) and 30 min (f). For comparison, the transient FTIR spectrum recorded by exposing 2%Zr/HZSM-5 to 1000 ppm NO + 10 % O_2 in N_2 at 250 ◦C for 30 min (dotted curve) was given as **m**

These results imply that the rate-determining step for the C_2H_2-SCR over HZSM-5 and HFER is the nitrous species formation from NO_x adsorption. Due to the restriction in length for the chapter, here, we will interpret only the rate-determining step of C_2H_2-SCR over HZSM-5 and HFER deduced from FTIR study on Zr and Y promoted zeolites.

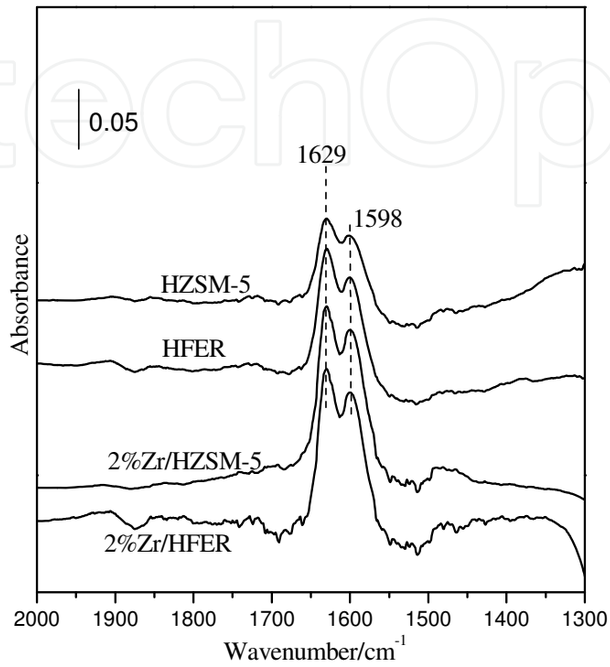

Fig. 10. FTIR spectra arising from surface nitrate species on HZSM-5, 2%Zr/HZSM-5, HFER, and 2%Zr/HFER upon the catalyst samples exposing to gas mixture of 1000 ppm NO + 10 % O_2 in N_2 for 30 min at 250 °C

The catalytic performance of HFER, HZSM-5, 2%Zr/HFER and 2%Zr/HZSM-5 in C_2H_2-SCR was shown in Fig. 8. The conversion of NO into N_2 was strongly influenced by the type of zeolites. The parent zeolite of HFER displayed much higher activity than HZSM-5 for C_2H_2-SCR in the temperature range of 250-375 °C. For instance, NO conversion to N_2 over HFER at 250 °C was 69.6%, which is much higher than that over HZSM-5 under the same reaction conditions. On the other hand, significant doping effect of zirconium incorporation into the zeolites on C_2H_2-SCR was observed, especially in the case of HZSM-5. For instance, NO conversion to N_2 was increased to 78.0% from 69.6% at 250 °C by 2% of zirconium incorporation into HFER, whereas it sharply increased to 56.0% from 25.4% in the case of HZSM-5. Why HFER was so much active at the lower reaction temperature compared to HZSM-5? Why the doping effect of zirconium on C_2H_2-SCR was so much larger for HZSM-5 than HFER? To answer these questions, we tentatively combined their catalytic performance in C_2H_2-SCR with their NO_x adsorption capacity. As shown in Fig. 9, Two bands at 1598 and 1629 cm^{-1} due to bidenate and bridging nitrates (Li et al., 2007; Tsyntsarski et al., 2003; Li et al., 2005a) respectively appeared on HZSM-5 and HFER when the zeolites were exposed to NO+O_2 at 250 °C. By comparing the band increasing in intensity at 1629 and 1598 cm^{-1} over the zeolites, it can be known that the nitrate species formation was faster over HFER than that over HZSM-5. Obviously, the relative nitrate species formation rate coincides well with

the relative C_2H_2-SCR activity for the two parent zeolites. Similar relationship of C_2H_2-SCR activity versus nitrate species formation rate can be also obtained on HZSM-5 and 2%Zr/HZSM-5. The bands due to nitrate species on 2%Zr/HZSM-5 (spectrum **m** in Fig. 9) were obviously strong in intensity compared to that obtained at the same exposing time over HZSM-5. Figure 10 gave the stable FTIR spectrum at 250 °C obtained by exposing HZSM-5, HFER, 2%Zr/HZSM-5 and 2%Zr/HFER respectively to gas mixture of 1000 ppm NO + 10 % O_2 in N_2 until the corresponding spectra no further change. By combining the results given in this figure with those in Fig. 8, the relative activity of the zeolites and those promoted by zirconium can be well understood. The lager nitrate species formation capacity of HFER compared to HZSM-5 may be the reason leading to the higher C_2H_2-SCR activity of HFER in comparison with HZSM-5. Accordingly, as 2%Zr/HFER have the further large nitrate species formation capacity, due to 2% of zirconium incorporation, it displayed more active than the zeolite itself. Also, the drastically larger C_2H_2-SCR activity of 2%Zr/HZSM-5 than that of the zeolite itself can be attributed to the substantially increased nitrate species formation capacity of the resulting material prepared from zirconium impregnation on the zeolite. To confirm the supposition that nitrate species formation on the catalyst surface is the rate-determining step for the C_2H_2-SCR over HZSM-5 and HFER, it must be validated that the nitrate species are important intermediate of the total reaction, i.e. they are active toward reduction, which will be discussed in the section 4. It should be also validated that, the step of nitrate species formation on the catalyst surface is most slow among all of the steps in the route of C_2H_2-SCR over the zeolites.

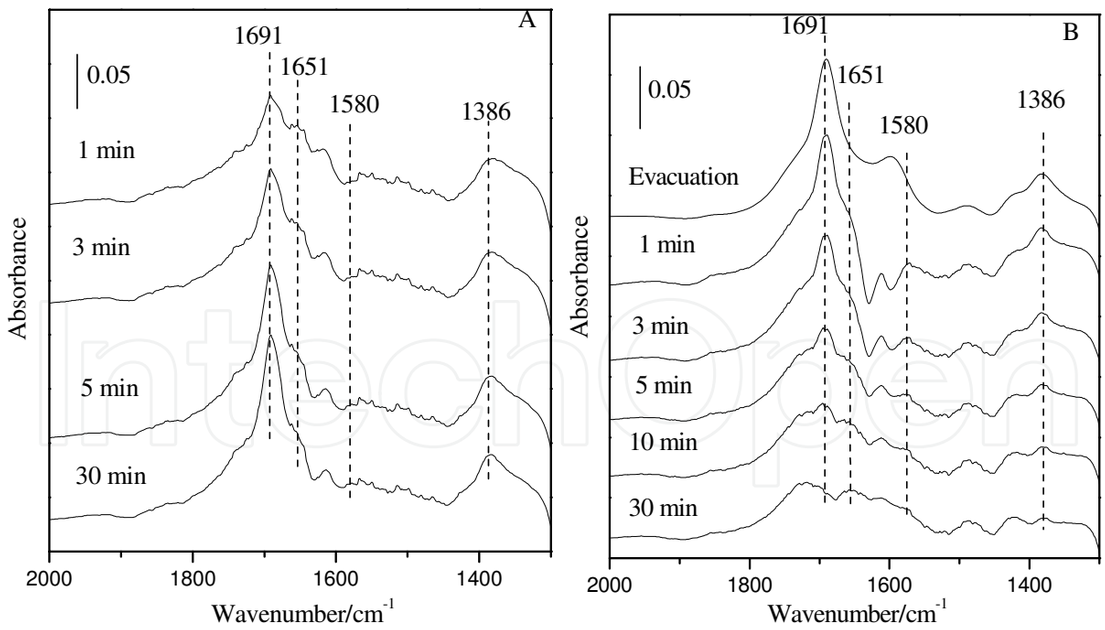

Fig. 11. FTIR spectra of surface species on HFER at 250 °C upon the fresh zeolite being exposed to 500 ppm C_2H_2 + 1000 ppm NO + 10 % O_2 in N_2 (A) and then to 1000 ppm NO + 10 % O_2 in N_2 (B)
Note: The cell was evacuated briefly before the zeolite was exposed to NO+O_2 in N_2

Figure 11 gave the transient in situ FTIR spectrum of surface species on HFER at 250 ^{o}C recorded when the zeolite was exposed to 500 ppm C_2H_2 + 1000 ppm NO + 10 % O_2 in N_2 and then reductant gas of acetylene was cut off thereafter. Although bands at 1598 and 1629 cm^{-1} due to nitrate species with strong intensity appeared in the spectra recorded when the zeolites were exposed to 1000 ppm NO + 10 % O_2 in N_2 (Fig.10), no one of them appeared in the transient in situ FTIR spectra as well as in the steady spectrum when 500 ppm C_2H_2 was introduced into the gas mixture, i.e. in the C_2H_2-SCR reaction condition. Furthermore, the nitrate species even could not be detected in the in situ FTIR in the followed period of 30 min (Fig 11B), even though C_2H_2 was completely removed out from the gas mixture. These experimental results indicate that no nitrate species (produced by NO+O_2 co-adsorption over the zeolite) can cumulate on the zeolite surface under the C_2H_2-SCR reaction condition. Instead, the species produced by adsorption of acetylene or its derivates obviously cumulated on the zeolite surface, being characterized by the bands at 1691, 1651 and 1380 cm^{-1}. It means that formation of the reductant species is faster by far than that required by nitrate species reduction. In other words, the rate of nitrate species reduction is limited by that of nitrate species formation. Thus, it can be concluded that the rate-determining step of C_2H_2-SCR over the HFER is the nitrate species formation step. Then, it can be further deduced that the C_2H_2-SCR reaction over HZSM-5 must be controlled also by this step, as discussed above, nitrate species formation capacity of HZSM-5 is much lower than that of HFER, and C_2H_2-SCR activity enhanced by zirconium impregnation was more significant on HZSM-5 than on HFER. Finally, it should be noted that, the quantitive evidence obtained by FTIR must be based on a strict experiment, e.g., the surface species must be measured over the self-supporting wafer with the same weight. Otherwise, accurate FTIR result may be hardly obtained. To compare the amount of surface species formed on the catalysts in FTIR, catalyst wafers with 14 ± 0.7 mg were selected and certain parameters of the IR spectrophotometer were set in our experiments.

4. To identify reaction intermediates

The identification of reaction intermediates is much important not only for investigating the reaction route over a catalyst, but also for understanding the effect of doping material being introduced to the catalyst. As motioned above, in the C_2H_2-SCR investigation, we found that Mo, W, Zr, Y impregnated on HZSM-5 and HFER significantly enhanced the formation of nitrate species over the catalyst and correspondingly increased the C_2H_2-SCR activity. These results could be well understood by the rate-determining step discussed in the section 3. On the other hand, we found that, NaZSM-5 is almost inactive for C_2H_2-SCR, though it can be considered that NaZSM-5 has much stronger nitrate species formation capacity compared to HZSM-5. Certainly, one can considered that due to lack of protons and inert for catalyzing NO oxidation, it can not initiate the aimed reaction. We also found that when NO in the gas mixture was completely changed to NO_2, the NO_2 conversion to N_2 over NaZSM-5 was still less much than that over HZSM-5. These results imply that NaZSM-5 hardly catalyzes C_2H_2-SCR due to not only inactive for NO oxidation, but also the other inferior action displayed in the subsequent steps. Thus, the role of protons in the NO reduction by acetylene over HZSM-5 was studied.

4.1 Characterization of nitrous species on HZSM-5 and NaZSM-5

The nitrous species formation and variation with temperature, as well as their reactivity towards to reduction by acetylene were investigated by FTIR. The spectra obtained upon

exposing HZSM-5 and NaZSM-5 to NO and O_2 at 40 °C were depicted in Fig. 12. On HZSM-5 (Fig.12 A), the bands at 1622 cm^{-1} due to weakly adsorbed NO_2 (Shimizu et al., 2001;

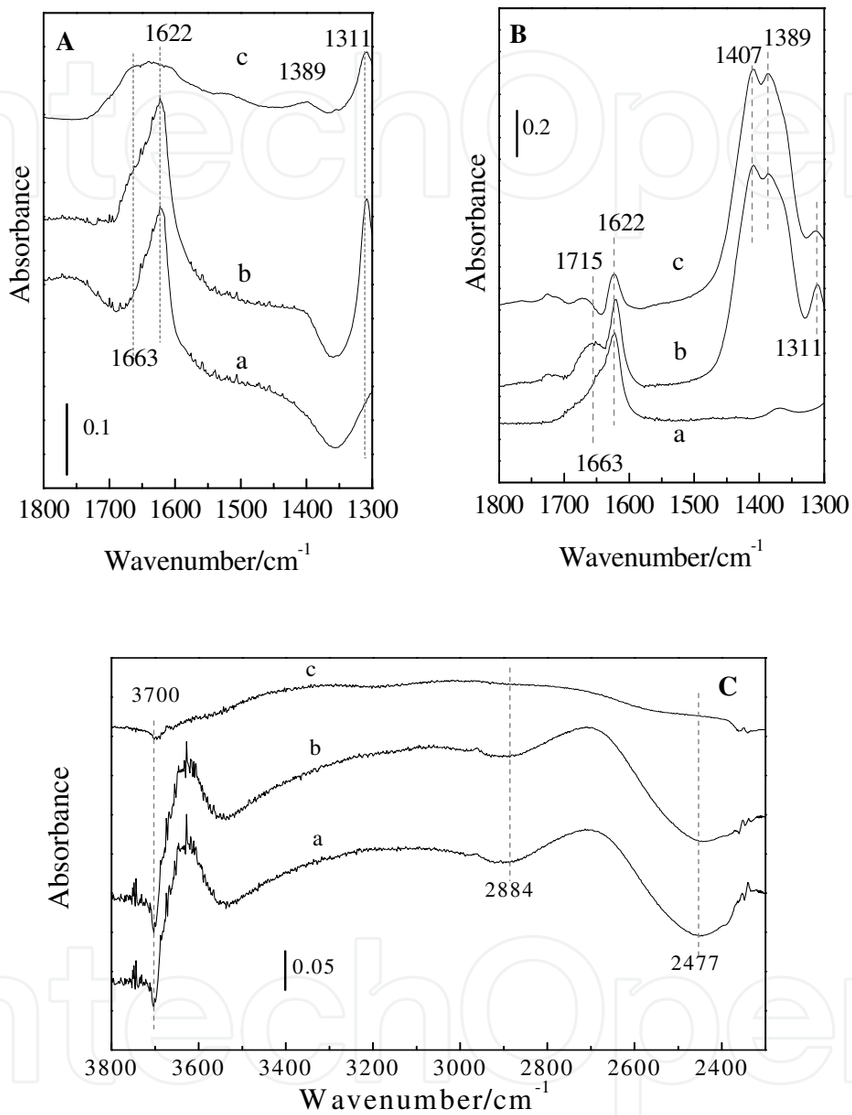

Fig. 12. FTIR spectra of surface nitrous species formed upon exposing HZSM-5 (A,C) and NaZSM-5 (B) to 1000 ppm NO and 10 % O_2 in N_2 at 40 °C for 1min (a), reaching saturated adsorption (b), and then a brief evacuation (c)

Pirngruber & Pieterse, 2006) or bridging nitrates (Ivanova et al., 2001; Yu et al., 2004; Sedlmair et al., 2003b; Li et al., 2005b) and that at 1311 cm^{-1} due to unidentate nitrates(Mihaylov et al., 2004; Shimizu et al., 2001; He et al., 2004) with three negative bands at 3700, 2884 and 2477 cm^{-1} were observed upon exposing the zeolite to NO+O_2 for 1 min. The band at 3700 cm^{-1} is due to asymmetric stretching vibration of molecular adsorbed water (Nakamoto, 1996;

Hadajiivanov et al., 1998), and the bands at 2884 and 2477 cm^{-1} are due to the well-known A-B-C structure produced by hydrogen-bonded hydroxyls (Mihaylov et al., 2004; Hadajiivanov et al., 1998). The results indicate that the formation of nitrates occurred at the expense of molecular adsorbed water through the reaction $2NO_2 + H_2O \rightarrow HNO_3 + HONO$ (Li et al., 2005b; Szanyi et al., 2004). Prolonged exposure of the sample to $NO+O_2$ led to an increase in intensity only at 1311 cm^{-1}, which can be explained by the reaction $M^{n+} - O^{2-} + 2NO_2 \rightarrow M^{n+} - NO_3^- + NO_2^-$ on cation defect sites such as extra-framework alumina, similar to the reaction pathway suggested by Larsen et al. (Li et al., 2005b). Part of the nitrous species (adsorbed NO_2 and some unidentate nitrates) corresponding to the bands at 1622 and 1311 cm^{-1} were so weakly adsorbed on the zeolite that they disappeared in the subsequent brief evacuation. At the same time, two bands at 1663 and 1389 cm^{-1} due to nitrites and/or nitrates associated with a very low concentration of Na^+ ions in HZSM-5 (Li. et al., 2005b; Satsuma et al., 1997; Szanyi & Paffett, 1996) were observed. Identical to HZSM-5, the band at 1622 cm^{-1} appeared rapidly with $NO+O_2$ co-adsorption on NaZSM-5 (Fig. 12B). However, different from HZSM-5, prolonged exposure of NaZSM-5 to $NO+O_2$ primarily resulted in the appearance of bands with strong intensity at 1407 and 1389 cm^{-1} due to nitrates banding to Na^+ (Li et al., 2005b; Satsuma et al., 1997; Szanyi & Paffett, 1999). It is clear by comparing Fig. 12 A and B that much more stable nitrous species could form on NaZSM-5 than on HZSM-5, which are in good accordance with the results obtained by NO_x-TPD as shown in Fig. 13. Thermal stability of the nitrous species on the zeolites was investigated by FTIR, as shown in Fig. 14. On HZSM-5, the band at 1311 cm^{-1} due to unidentate nitrates disappeared at 150 °C, and a band appeared at 1585 cm^{-1} due to bidentate nitrates (Ivanova et al., 2001; Yu et al., 2004; Shimizu et al., 2001; He et al., 2004; Poignant et al., 2001). It indicates that the bidentate nitrates were produced from unidentate nitrates at the elevated temperature. Compared with the bridging nitrates (1622 cm^{-1}), the bidentate nitrates (1585 cm^{-1}) were more thermally stable; the intensity at 1585 cm^{-1} slightly decreased with the temperature increasing. Similar to those on HZSM-5, unidentate nitrates

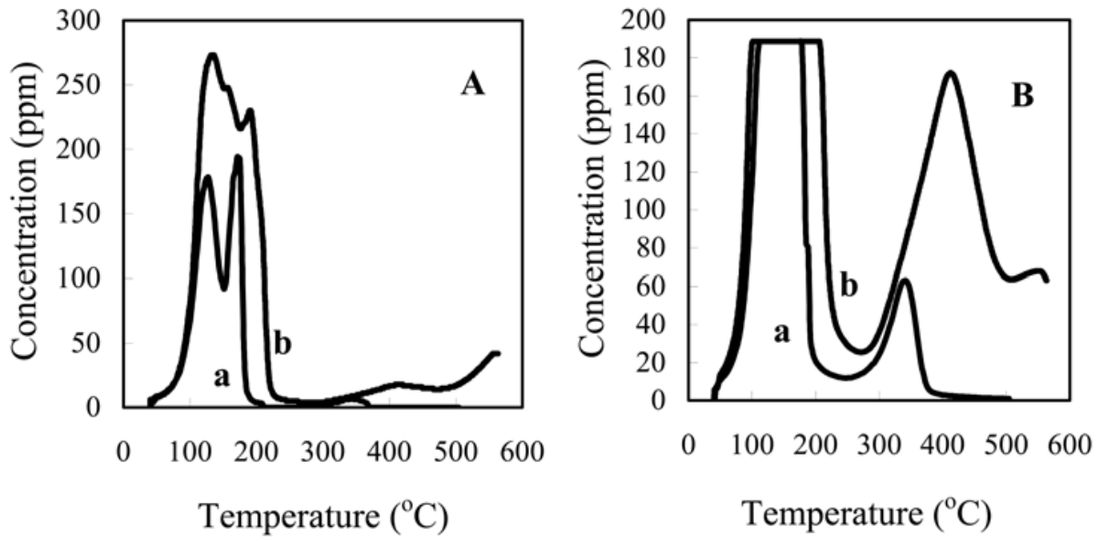

Fig. 13. TPD profiles of NO (A) and NO_2 (B) in N_2 flow after saturated co-adsorption of $NO+O_2$ on HZSM-5 (a) and on NaZSM-5 (b)

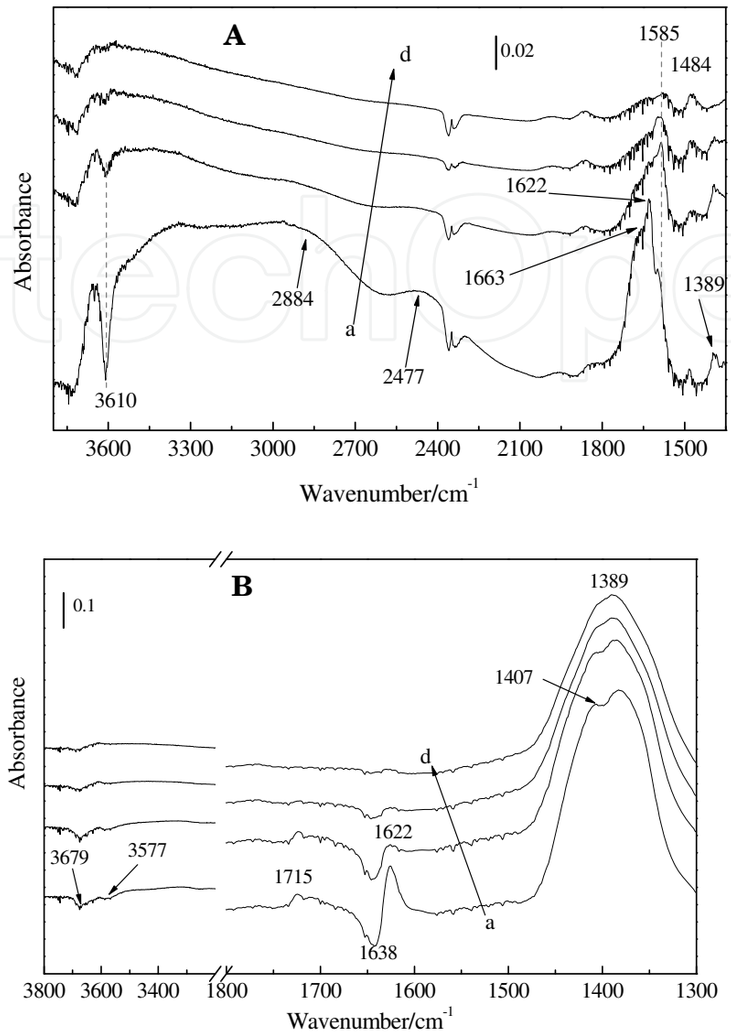

Fig. 14. The nitrous species on HZSM-5 (A) and on NaZSM-5 (B) at 150 °C (a), 250 °C (b), 350 °C (c) and 400 °C (d)

(1311 cm^{-1}) on NaZSM-5 disappeared at 150 °C, indicating that the unidentate nitrate species are less thermal stable than the other kinds of nitrates, irrespective of the adsorbents. It implies that the unidentate nitrates are not involved in the C_2H_2-SCR, as the reaction significantly occurred at the temperature above 250 °C. Quite different from the findings on HZSM-5, although the bridging nitrates (giving band at 1622 cm^{-1}) on NaZSM-5 changed little at 150 °C, most of them desorbed when the temperature increased to 250 °C. Band at 1715 cm^{-1}, observed exclusively on NaZSM-5, could be assigned to nitrates associated with Na^+ ions, because it appeared concomitantly with the band at 1407 cm^{-1} during the co-adsorption of NO+O_2 (Fig. 12 B) and disappeared at 350 °C together with the same band (Fig. 14). On NaZSM-5, the most stable nitrous species are the nitrate species associated with Na^+ (1389 cm^{-1}), which could remained on the zeolite at 400 °C. The FTIR results reveal that the adsorption of NO_x on ZSM-5 was strongly affected by the cations in the zeolite, and that protons were essential for the bidentate nitrates formation on the zeolites.

4.2 Characterization on the activity of nitrous species towards to reduction on the zeolites

The bands due to nitrate species at 1626 and 1585 cm^{-1} disappeared within 1 min upon exposure of HZSM-5 to C_2H_2+O_2 at 250 ◦C (Fig. 15A). Concomitantly, the bands at 1693 cm^{-1} due to carbonyl-containing compound and at 1605 cm^{-1} due to the C=O vibration of carboxylic groups (Li et al., 2005b) appeared. It indicates that the bridging and bidentate nitrates are very active with reductant. However, no significant change in the spectra was observed when the NaZSM-5 was exposed to the gas mixture of C_2H_2+O_2 at 250 ◦C, as shown Fig. 15 B), indicating that the nitrate species bonding to Na^+ on NaZSM-5 are inert to the reductant. The quite different nitrous species formed on HZSM-5 and on NaZSM-5 as well as their disparate reactivity with reductant could explain the distinct catalytic performance of the two zeolites in C_2H_2-SCR. Thus, it is rational to draw the conclusion that protons are responsible not only for catalyzing NO oxidation to NO_2, but also for the formation of active nitrate intermediates in the C_2H_2-SCR.

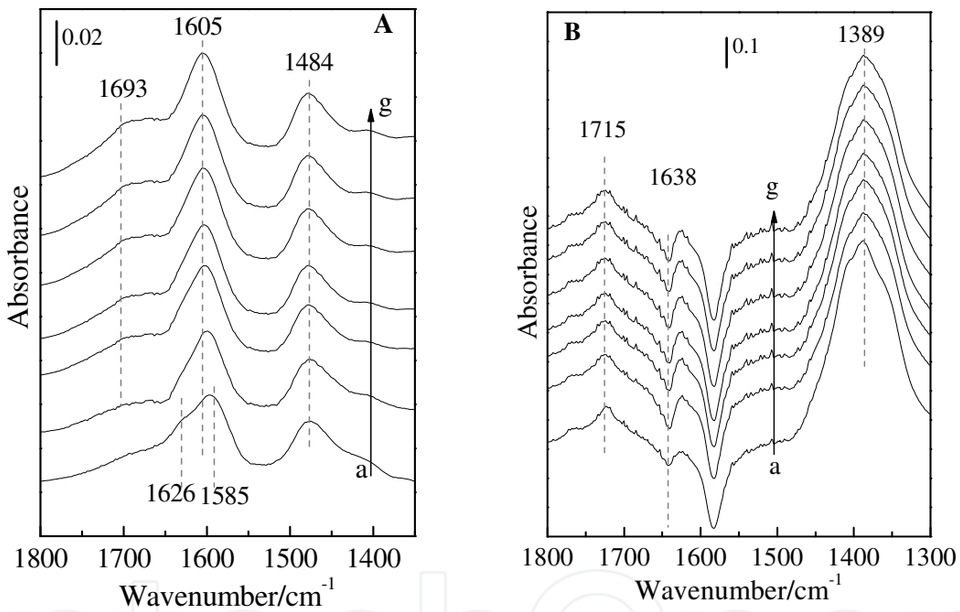

Fig. 15. FTIR spectra of surface species on HZSM-5 (A) and NaZSM-5 (B) at 250 ºC when the zeolite was subjected to saturated coadsorption of NO+O_2 and a subsequent brief evacuation (a), and then an exposure to C_2H_2+O_2 for 1 min (b), 2 min (c), 4 min(d), 6 min (e), 8 min (f), and 10 min (g)

4.3 Characterization of carbonous species and the reactivity with nitrous species on the zeolites

The evolution of carbonous species and their reactivity toward NO_x were investigated by FTIR. The IR spectra of carbonous species due to saturated adsorption of acetylene on the HZSM-5 and NaZSM-5 at 80 ◦C are depicted in Fig. 16. The adsorption of acetylene on HZSM-5 resulted in the appearance of positive bands at 1673 and 1628 cm^{-1} and negative bands at 3700, 2884, and 2477 cm^{-1} (Fig. 16, spectrum c). As discussed in Section 4.1, the three negative bands are arisen from the consumption of adsorbed water on the Brønsted

acid site. No negative band at 3610 cm^{-1} due to consumption of acidic zeolite Al(OH)Si hydroxyls (Poignant et al., 2001; Brosius et al., 2005) was observed caused by acetylene adsorption. In an energy standpoint, acetylene would adsorb on the free Brønsted acid sites, which were characterized by band at 3610 cm^{-1} as shown in Fig. 17, rather than adsorb on the ones taken up by water. Therefore, it is reasonable to propose that acetylene reacted with the adsorbed water on the Brønsted acid site, but did not simply take up the Brønsted acid site by breaking the well-known A–B–C structure.

Based on above conclusion that acetylene reaction with water on Brønsted acid sites when adsorbed on HZSM-5, it can be further reasonably speculated that vinyl alcohol (CH_2=CH–OH) species were formed by acetylene adsorption on the zeolite as depicted by model 1 as shown in scheme 1: In principle, acetylene can be adsorbed on ZSM-5 in two ways. One way does by reacting with water to form vinyl alcohol and the later can be strongly bonded to Brønsted acid sites with hydrogen bond (model I), being characterized by a blue shift of ν(C=C) with respect to the general C=C double band. Due to hydrogen bond of the –OH group with the Brønsted acid sites, the blue shift of ν(C=C) may be further aggravated, and it is the primary case of acetylene adsorption on HZSM-5, which is strongly supported by the band of 1628 and 1723 cm^{-1}. Another way does by binding to the cations (e.g. H^+ and Na^+) in zeolite channels through weak static attraction to form a π-complex, which may decreases the electron density in the highest occupied molecular orbital, leading to a red shift of ν(C=C) with respect to the general C=C double band (model II). Obviously, it is the primary case of acetylene adsorption on NaZSM-5, which is strongly supported by the band at 1621 cm^{-1}.

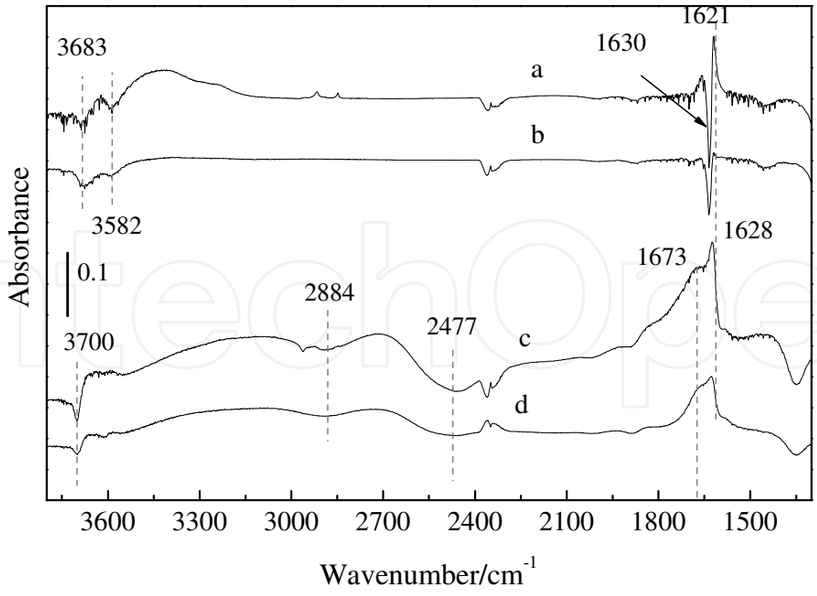

Fig. 16. FTIR spectra of carbonous species formed by saturated adsorption of C_2H_2 (500 ppm) in N_2 at 80 °C on NaZSM-5 (a), HZSM-5 (c), and those when the sample of NaZSM-5 (b) and HZSM-5 (d) was subsequently subjected to a brief evacuation at this temperature

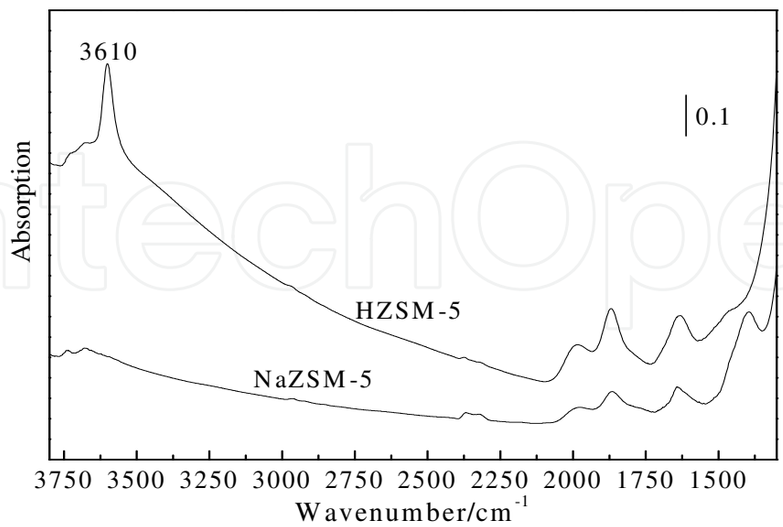

Fig. 17. FTIR spectra of fresh HZSM-5 and NaZSM-5

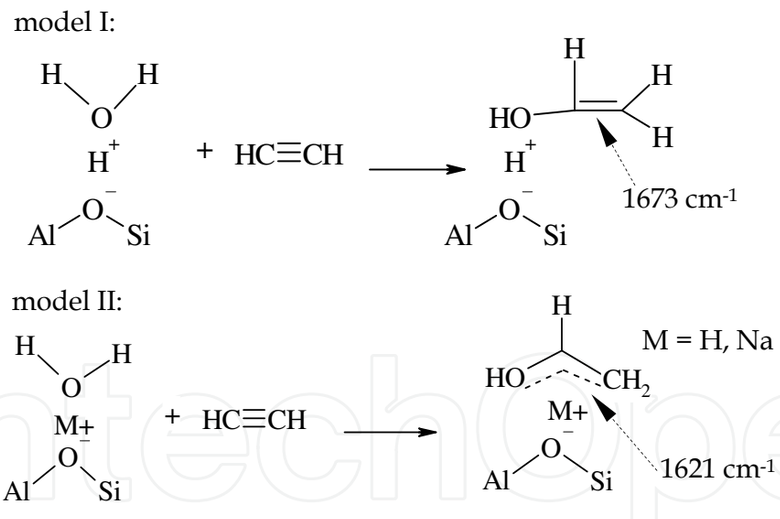

Scheme 1. C_2H_2 adsorption model on the HZSM-5 and NaZSM-5

Evolution of the carbonous species on HZSM-5 with temperature is shown in Fig. 18. It is obvious that the intensity of the band at 3659 cm^{-1} due to ν(–OH) of alcohol hydroxyl groups increased with the temperature increase from 80 to 150 °C. At the same time, the bands at 2884 and 2477 cm^{-1} due to the A–B–C structure, and the band at 1352 cm^{-1} due to δ(OH) of the H-bonded zeolite hydroxyls were recovered on the HZSM-5 (Fig. 18), accompanied by the appearance of the negative band at 3610 cm^{-1}. With the temperature further increase, the bands relating to adsorbed water on the Brønsted acid sites increased in

intensity. It indicates that water was formed and adsorbed on the Brønsted acid sites at elevated temperatures. Above 300 °C, the strong band centered at 1628 cm^{-1} disappeared, which correlates well with the end of desorption peak (around 215 °C) of acetylene in C_2H_2-TPD (not shown). As a result, a new band at 1646 cm^{-1} was clearly observed. Based on these results, a scheme 2 for the evolution of carbonous species with temperature on HZSM-5 can be proposed.

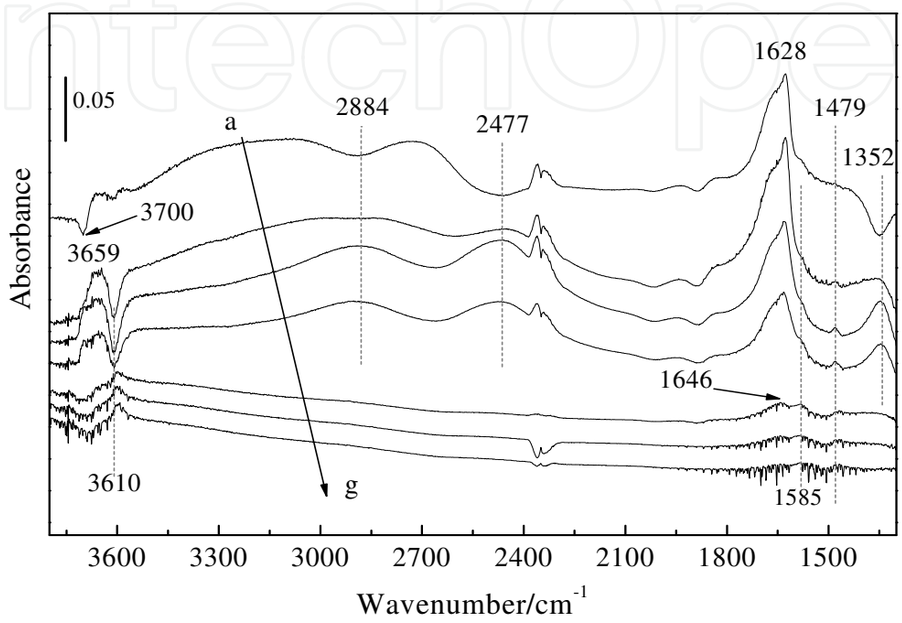

Fig. 18. Spectra of carbonous species on HZSM-5 when evacuated at 80 °C (a), at 150 °C (b), at 178 °C (c), (d) at 200 °C (d), at 300 °C (e), at 360 °C (f), and at 410 °C (g) after saturated adsorption of acetylene

The vinyl alcohol adsorbed on the Brønsted acid sites in the models both I and II was converted to a carbenium ion ($HO–HC^+–CH_3$), which gave bands at 3659 and 1352 cm^{-1} due to the OH stretching vibration and the CH_3 deformation vibration, respectively. The carbenium ion decomposed to water and another carbonium ion ($CH_2=HC^+$) that gave the band at 1646 cm^{-1}. The formed water adsorbed on Brønsted acid sites led to a recovery of intensity and an increase of the bands at 2884 and 2477 cm^{-1}, as well as the negative band at 3610 cm^{-1}. In addition, some of the carbenium ion ($HO–HC^+–CH_3$) was oxidized by oxygen (ca. 5000 ppm) in the pure N_2 (99.995%) to acetate species, giving the bands at 1585 and 1479 cm^{-1} due to the νas(COO) and νs(COO) of acetate species (Yu et al., 2004; Shimizu et al., 2001; He et al., 2004; Poignant et al., 2001; Wu et al., 2005).

Evolution of the carbonous species on HZSM-5 with temperature is shown in Fig. 19. Temperature increase from 80 to 200 °C resulted in recovery of the band at 1635 cm^{-1} as well as a shift of the band (from 1623 to 1628 cm^{-1}). Scheme 3 explains that acetylene was released by the decomposition of vinyl alcohol, leaving water on the cation sites in zeolite, leading to the disappearance of the negative band. Above 300 °C, almost no carbonous surface species were detected on Na-ZSM-5, which is in line with the results obtained in C_2H_2-TPD (not shown).

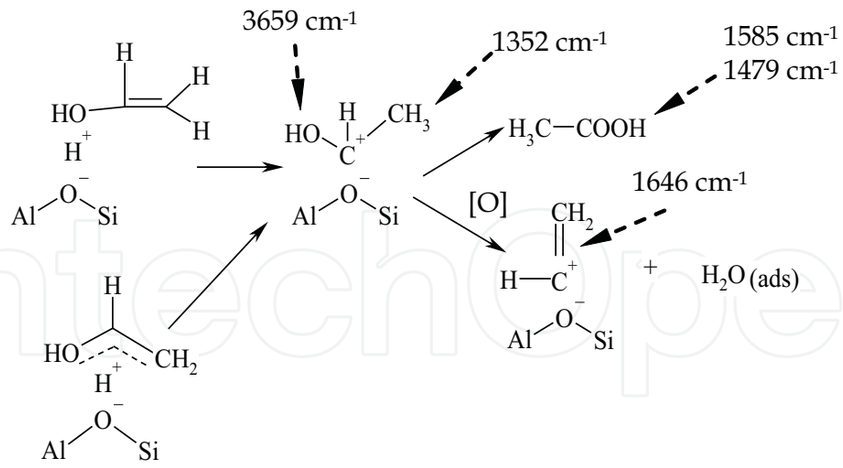

Scheme 2. The evolution of carbonous species on HZSM-5

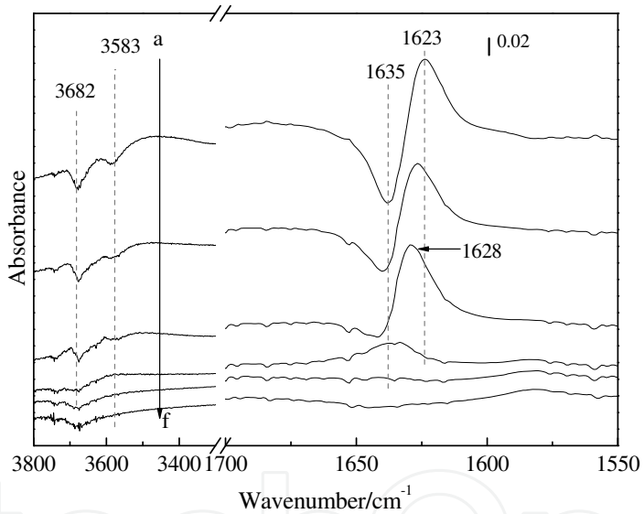

Fig. 19. Spectra of carbonous species on NaZSM-5 when evacuated at 150 °C (a), at 178 °C (b), at 200 °C (c), (d) at 300 °C (d), at 360 °C (e), and at 420 °C (f), after saturated adsorption of acetylene

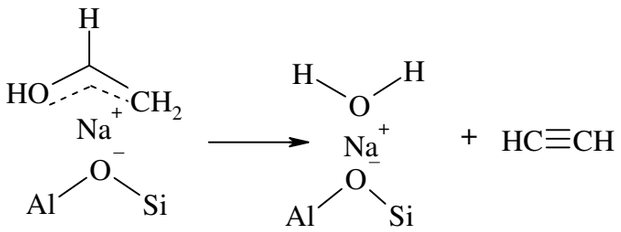

Scheme 3. The decomposition of carbonous species on NaZSM-5

The reactivity of carbonous species on HZSM-5 and on NaZSM-5 with NO and NO+O_2 was studied at 200 °C. Acetate species (1585, 1479 cm^{-1}) were detected at steady state on HZSM-5 in NO/N_2 and N_2 (Fig. 20 A), indicating that the acetate species could exist in NO/N_2. This means that acetate species did not react with NO at the temperature. However, in NO+O_2/N_2, no acetate species could be detected, and instead, a new band at 2131 cm^{-1} appeared. This band can be assigned to ν(C≡N) of cyanide (Shimizu et al., 2001; Mosqueda-Jiménez et al., 2003b) produced by the reaction of acetate species with NO_x. The result indicates that the acetate species formed by carbenium ion ($HO–HC^+–CH_3$) oxidation on HZSM-5 are active with nitrous species arising from the co-adsorption of NO+O_2. Thus it can be reasonably considered that acetate species is one of the important intermediates for the C_2H_2-SCR. In contrast to the case of HZSM-5, although vinyl alcohol (1628 cm^{-1}) was also formed on NaZSM-5 (Fig. 20 B), no significant change of the band in intensity was observed when the gas mixture was switched form NO/N_2 to NO+O_2/N_2, indicating that the vinyl alcohol bonding to Na^+ in NaZSM-5 is inert under the reaction conditions.
Based on above discussion, it is clear that, the carbonous species formed by acetylene adsorption on HZSM-5 and on NaZSM-5 as well as their reactivity with nitrous species are also quite different.

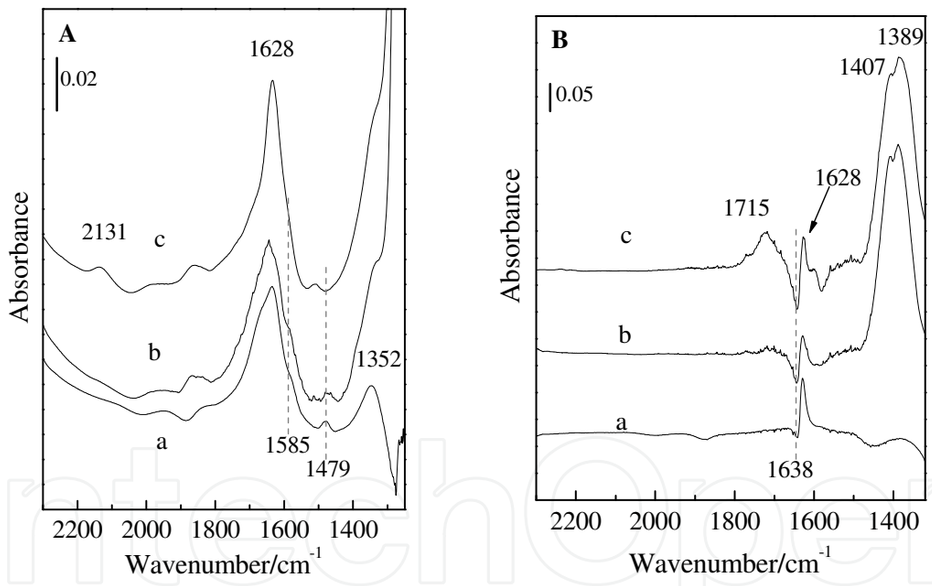

Fig. 20. FTIR spectra of surface species on HZSM-5 (A) and NaZSM-5 (B) at 200 °C taken in (a) N_2, (b) NO, (c) NO + O_2. Before the measurements, the catalysts were pretreated in C_2H_2/N_2 at 80 °C

5. To propose possible reaction mechanism

To design a catalyst more active for the HC-SCR in real lean-burn conditions, extensive studies were also carried out on mechanism of the reaction. There have been different opinions concerning the mechanism of HC-SCR in literature, which can be roughly classified as "dissociative" (Goula et al., 2007; Burch & Watling, 1996) and "reduction" ones

(Mihaylov et al., 2004; Mosqueda-Jiménez et al., 2003b; Hadjiivanov et al., 2003). The "dissociative" mechanism proposed by Burch and Watling (Burch & Watling, 1996) has been widely accepted by the authors being concerned with noble metal catalysts in the HC-SCR field, and it can be expressed as follows (Goula et al., 2007):

$$NO_{ads} \rightarrow N_{ads} + O_{ads} \quad (1)$$

$$N_{ads} + N_{ads} \rightarrow N_2(g) \quad (2)$$

$$N_{ads} + NO_{ads} \rightarrow N_2O(g) \quad (3)$$

For the "reduction" mechanism of HC-SCR, some authors have claimed that activation of hydrocarbon occurs first, and some partially oxidized hydrocarbons ($C_xH_yO_z$) produced by the step then react with NO and/or NO_2 to form the secondary intermediates (Sasaki et al., 1992). For example, formate and acetate were proposed to be active species of HC-SCR over CoO_x/Al_2O_3 (He & KÖhler, 2006), Ga_2O_3/Al_2O_3 (He et al., 2005), Ag/Al_2O_3 (Shibata et al., 2003), SnO_2/Al_2O_3 (Liu et al., 2006), $Cu\text{-}Al_2O_3$ (Shimizu et al., 2000; Satsuma & Shimizu, 2003), In_2O_3/Al_2O_3 (Luo et al., 2007), Ag/Al_2O_3 (Zhan et al., 2007) and Pd/Al_2O_3 catalysts (Huuhtanen et al., 2002). Acetaldehyde deriving from propene was also proposed to be main active species of the HC-SCR over sulfated titania-supported rhodium catalyst (Flores-Moreno et al., 2005). However, some authors have claimed that activation of NO_x occurs first, forming nitrous surface species, such as nitro (Meunier et al., 2000), nitroso (Poignant et al., 2001, Gerlach et al., 1999), nitrosonium ions (Gerlach et al., 1999, Ingelsten et al., 2005), nitrate or nitrite (Luo et al.,2007, Anunziata et al., 2007) over the catalyst. For instance, bridging and bidentate nitrates were reported to be produced first by co-adsorption of $NO+O_2$ on $Co/SO_4^{2-}\text{-}ZrO_2$ (Tsyntsarski et al., 2003), BaY (Sedlmair et al., 2003a) and Ag/Al_2O_3 (Bentrup et al., 2005). Tsyntsarski et al. (Tsyntsarski et al., 2003) have suggested that both bridging and bidentate nitrates are active species of the HC-SCR. Mihaylov et al. (Mihaylov et al., 2004) have reported that monodentate nitrates on Ni-HZSM-5 are highly reactive towards methane. Lónyi et al. (Lónyi et al., 2007) have studied selective catalytic reduction of NO by CH_4 over Co-, Co,Pt-, and H-mordenite catalysts and suggested that nitrosonium ions are surface intermediates of the reaction. There are also some other suggestions about the reaction intermediate of HC-SCR in literature, including nitrile (Poignant et al., 2001; Delahay et al., 2007), isocyanate (Mihaylov et al., 2004; Mosqueda-Jiménez et al., 2004b; He & KÖhler, 2006), R-NO_x (Mosqueda-Jiménez et al.,2003; Cowan et al., 1998), amine (Poignant et al., 2001), acetonoxime (Shimizu et al.,2000; Resini et al., 2003) and ammonia (Lónyi et al., 2007).

Although most of the "reduction" mechanisms were supported by Fourier transform infrared (FTIR) identification of reaction intermediates (Joubert et al., 2006), none of them has been widely accepted because of the complexity of the process (Mosqueda-Jiménez et al., 2003b) being concerned with different catalysts, reductants and reaction conditions. More investigation on the reaction mechanism is required for understanding the real reaction route of HC-SCR over different catalysts and using different reductants.

5.1 Reaction mechanism of C_2H_2-SCR over Mo/HMOR

In the this section, a possible reaction mechanism of C_2H_2-SCR over Mo/ HMOR （Li et al., 2008） and Zr/HFER (Xing et al., 2008) investigated by in situ FTIR was summarized.

Fig 21 shows conversion of NO and C_2H_2 in C_2H_2-SCR over the mordenite-based catalysts (HMOR, 0.5%Mo/HMOR, NaMOR) as a function of temperature. The activity of 0.5%Mo/HMOR for C_2H_2-SCR was considerably high compared to HMOR and NaMOR. 70% of NO conversion to N_2 at 350 ^oC over 0.5% Mo/HMOR catalyst was obtained. It indicates that molybdenum has a significant promotional effect on C_2H_2-SCR. The peak of the "volcano" curve in NO conversion to N_2 versus reaction temperature seems to be in line with the temperature where C_2H_2 was nearly completely consumed. Hence, the drop of NO conversion above 350 ^oC can be considered to be caused by the lack of reductant.

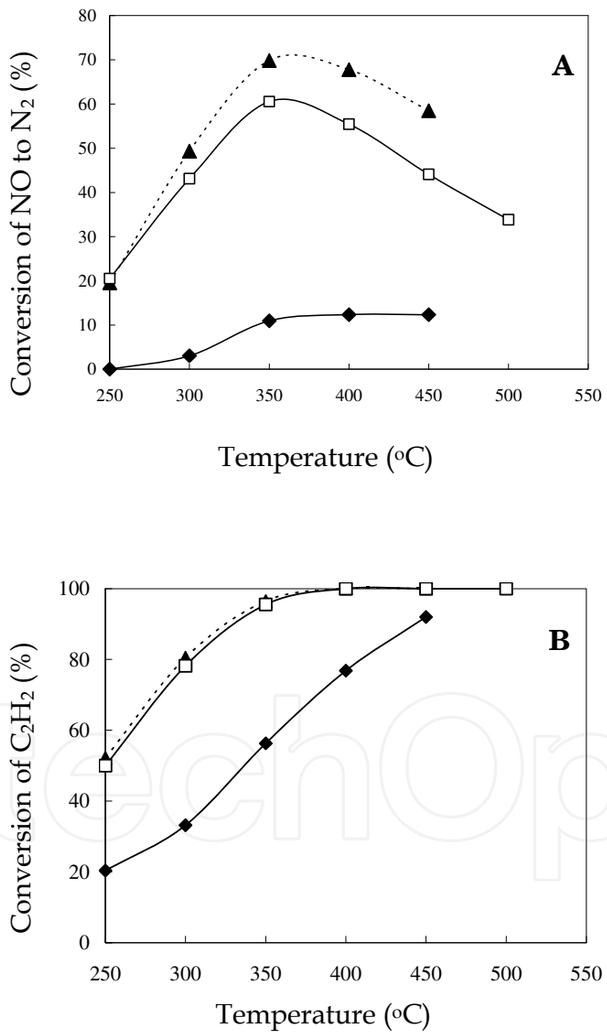

Fig. 21. Conversion of NO (A) and C_2H_2 (B) as a function of reaction temperature in C_2H_2-SCR. Reaction condition: 1600 ppm NO, 800 ppm C_2H_2, 9.95 % O_2 in He with a total flow rate of 50 ml/min over HMOR 0.100 g (□), 0.5 % Mo/HMOR 0.100 g (▲) or NaMOR 0.200 g (♦)

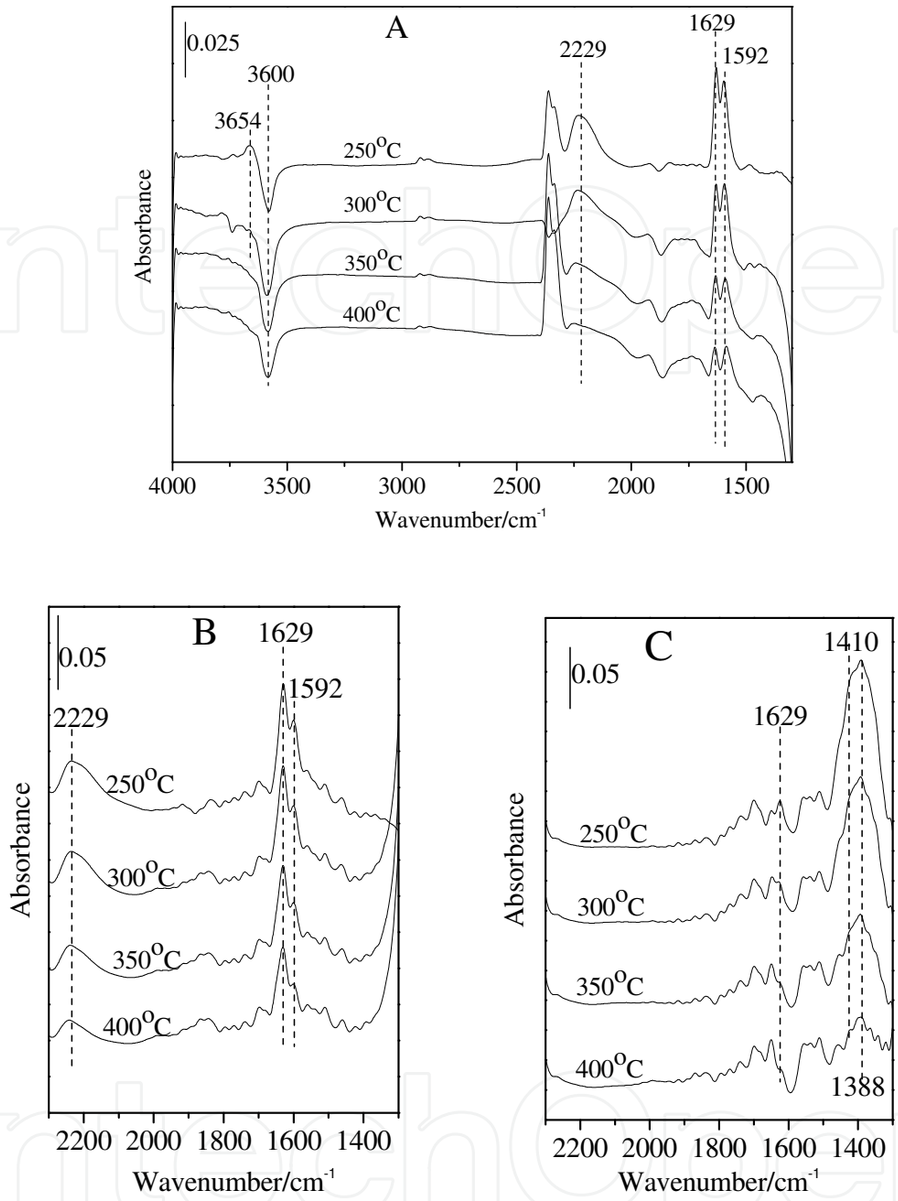

Fig. 22. Steady state in situ FTIR spectra of surface species on HMOR (A), 0.5%Mo/HMOR (B) and NaMOR (C) in 1000 ppm NO + 10% O_2 + N_2 at different temperature

Figure 22 shows steady state in situ FTIR spectra of nitric species formed by NO+O_2 co-adsorption on the mordenite-based catalysts at different temperatures. Three main bands at 2229, 1629 and 1592 cm^{-1} associated with nitric species were observed on HMOR (Fig. 22 A). The band at 2229 cm^{-1} is due to N-O stretching mode in NO^+ (Li et al., 2005a; Pirngruber & Pieterse, 2006; Gerlach et al., 1999), and the bands at 1629 and 1592 cm^{-1} can be assigned to bridging and bidentate nitrates (Poignant et al., 2001; Li et al., 2005a; Sedlmair et al., 2003; Yu et al., 2007), respectively. The NO^+ (2229 cm^{-1}) species was also detected by Gerlach et al. (Gerlach et al., 1999) at 120 °C when NO_x was adsorbed on the zeolite. As shown in Fig. 22

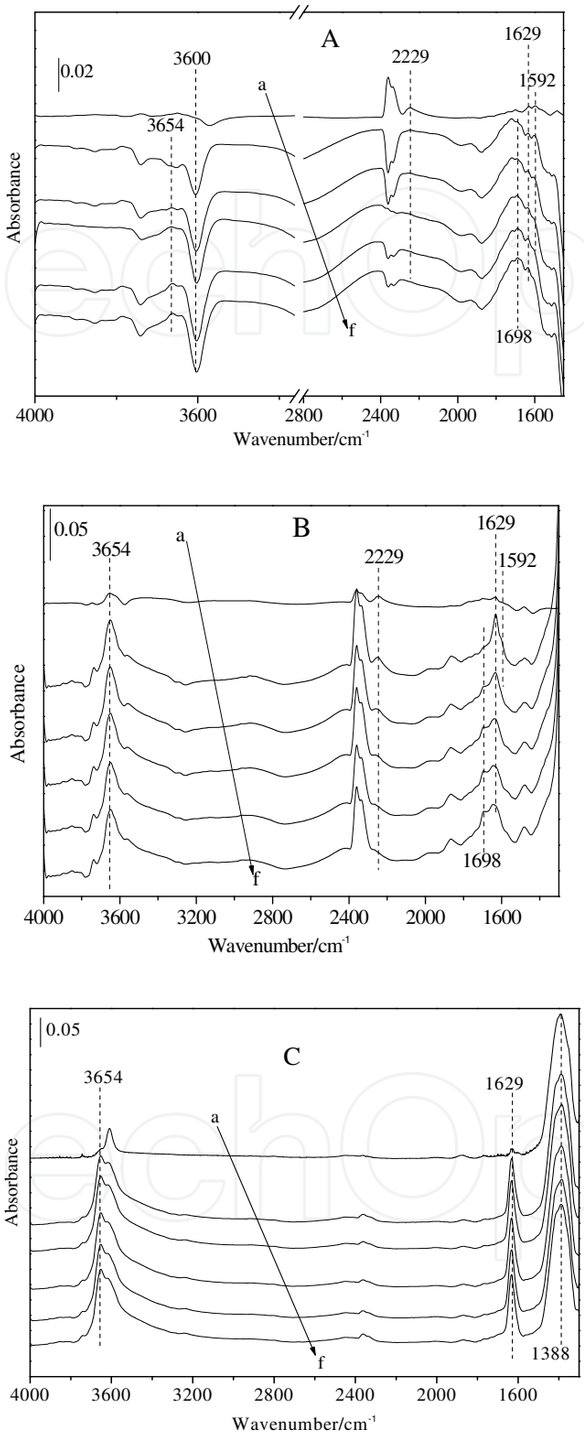

Fig. 23. In situ FTIR spectra on HMOR (A), 0.5%Mo/HMOR (B) and NaMOR (C) at 250 ^{o}C: a brief evacuation after saturated adsorption of NO+O_2 (a), and subsequently exposing to C_2H_2+O_2 for: 1 min (b), 3 min (c), 5 min (d), 8 min (e), 30 min (f)

A, a positive band at 3654 cm^{-1} due to adsorbed water (Mihaylov et al., 2004; Chafik et al., 1998) and a negative band at 3600 cm^{-1} due to Brønsted acid sites (Mihaylov et al., 2004; Gutierrez et al.,2007) were observed after co-adsorption of NO and O_2 on the zeolite at 250 ^oC. It can be well interpreted by the NO^+ formation pathway $NO + NO_2 + 2H^+ \rightarrow 2NO^+ + H_2O$, proposed by Hadjiivanov et al. (Hadajiivanov et al., 1998) and Gerlach et al. (Gerlach et al., 1999). Band at 1629 cm^{-1} due to bridging nitrate and band at 2229 cm^{-1} due to NO^+ on 0.5%Mo/HMOR are obviously greater in intensity respectively compared with those on HMOR, particularly above 300 ^oC (Fig. 22 B). It indicates that molybdenum loading on the HMOR zeolite have a promotional effect on the nitric species formation at higher temperature. On NaMOR (Fig. 22 C), band (1629 cm^{-1}) due to this type of bridging nitrate was rather weak, and bands due to bidentate nitrates (1592 cm^{-1}) and NO^+ species (2229 cm^{-1}) even could not be observed. Instead, a broad band at 1410-1388 cm^{-1} due to nitrate ions attached to Na^+ sites (Mihaylov et al., 2004; Li et al., 2005a; Yu et al., 2007) appeared after $NO+O_2$ co-adsorption on the sample under the same condition.

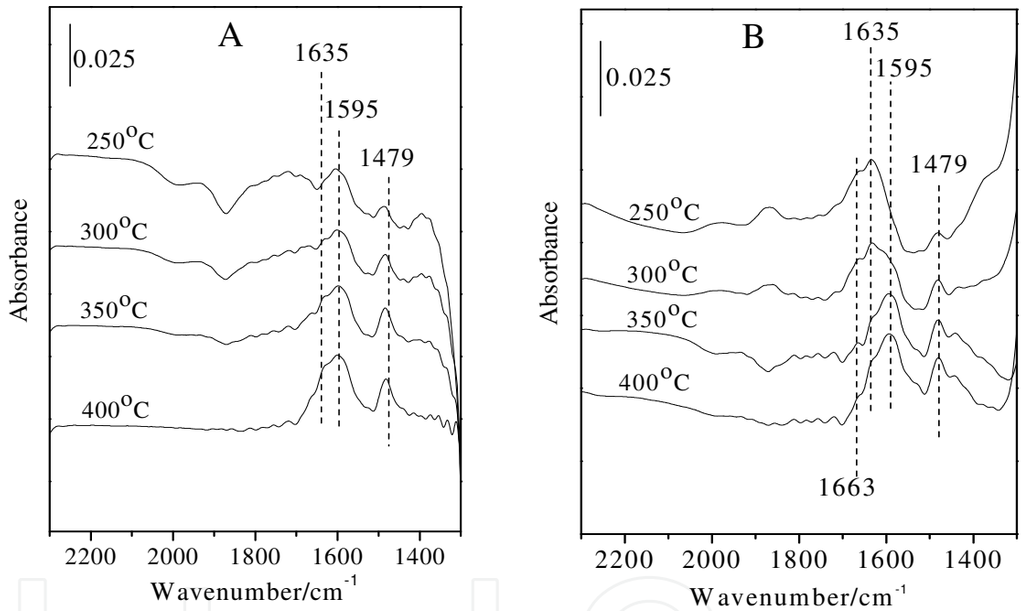

Fig. 24. Steady state in situ FTIR spectra of adsorbed species in 500 ppm C_2H_2 + 10 % O_2 + N_2 on HMOR (A), 0.5 % Mo/HMOR (B) at different temperature

Reactivity of the nitric species towards $C_2H_2+O_2$ over the mordenite-based catalysts was examined by in situ FTIR at 250 ^oC (Fig. 23). When $C_2H_2+O_2$ was introduced into the FTIR cell, bands due to bidentate nitrates (1592 cm^{-1}) and NO^+ species (2229 cm^{-1}) on HMOR arisen from $NO+O_2$ pre-adsorption (Fig. 23A) rapidly decreased. Concomitantly, a new band at 1698 cm^{-1} appeared and reached its maximum intensity within 3 min with disappearance of bands at 2229 and 1592 cm^{-1}. Similar result was obtained when C_2H_2 was used instead of $C_2H_2+O_2$ in the above experiment. The results indicate that NO^+ and bidentate nitrate species are fairly reactive towards acetylene at this temperature. It was evidenced by the following changes of bands associated with water formation during the process: A positive band at 3654 cm^{-1} due to water appeared, and at the same time, a negative band at 3600 cm^{-1} arisen from water adsorption on Brønsted acid sites

correspondingly increased in intensity. Unfortunately, the corresponding reactivity of bridging nitrate species (1629 cm^{-1}) could not be directly evaluated on the zeolite because of water formation. The band due to bending mode of water appears at the identical wave number with that of bridging nitrate species at 1629 cm^{-1}. Similar experimental results as that on HMOR was obtained on 0.5%Mo/HMOR (Fig. 23 B). However, quite different results were obtained on NaMOR. The nitrate species attached to Na^+ seem to be completely inert towards the reactant. No change in intensity of band at 1388 cm^{-1} due to the species could be observed on NaMOR (Fig. 23 C). Meanwhile, as expected, band at 1698 cm^{-1} did not appear on NaMOR. Instead, strong bands at 3654 and 1629 cm^{-1} due to water adsorbed on the Na-form zeolite were observed, which may be simply resulted from combustion of acetylene.

Figure 24 shows steady state in situ FTIR spectra of the surface species on HMOR and on 0.5%Mo/HMOR in gas mixture of 500 ppm C_2H_2 + 10% O_2/N_2 at different temperatures. No band at 1698 cm^{-1} could be observed on the catalysts. Instead, bands at 1635, 1595 and 1479 cm^{-1} due to ν(C=O), ν_{as}(COO) and ν_s (COO) of carboxylic groups (Hadajiivanov et al., 1998; Shimizu et al., 2007) appeared. Combined the result with that observed in Fig. 23, the band at 1698 cm^{-1} can be attributed to nitrogen containing organic species, because this band could appear only in the following conditions: both the nitric species (nitrogen oxides and/or nitric surface species) and the reductant were present together in the reaction system.

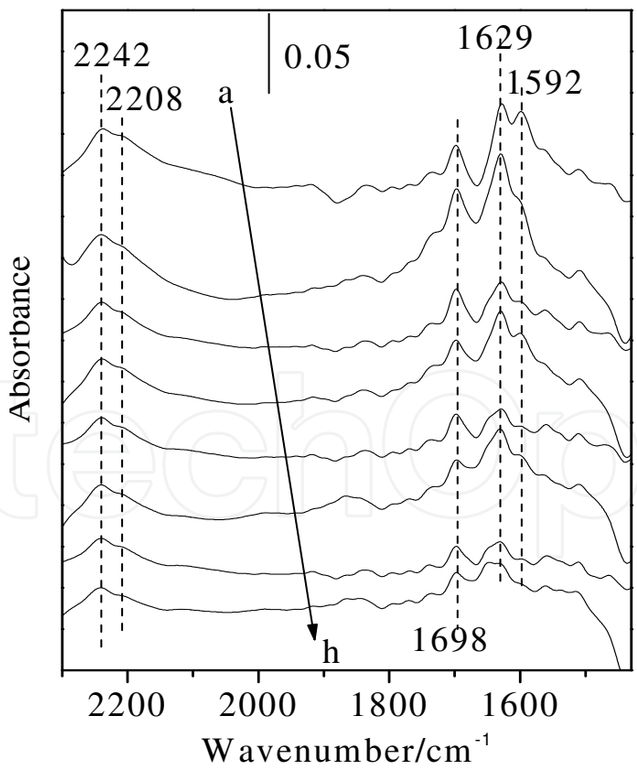

Fig. 25. Steady state in situ FTIR spectra of adsorbed species on 0.5%Mo/HMOR in gas mixture of 1000 ppm NO + 500 ppm C_2H_2 + 10 % O_2 + N_2 at 250 °C (a), 300 °C (c), 350 °C (e), 400 °C (g) and that on HMOR at 250 °C (b), 300 °C (d), 350 °C (f), 400 °C (h)

Figure 25 shows the steady state in situ FTIR reaction spectra of the surface species on HMOR and 0.5%Mo/HMOR in gas mixture of 1000 ppm NO + 500 ppm C_2H_2 + 10% O_2/N_2 at different temperatures. Two overlapped bands respectively centered at 2242 and 2208 cm^{-1} were appeared in the spectra, in addition to the bands at 1698, 1629 and 1592 cm^{-1}. The band at 2242 cm^{-1} can be assigned to -NCO vibration of isocyanate (2242 cm^{-1}) (Satsuma & Shimizu, 2003; Kameoka et al., 2000) and that at 2208 cm^{-1} can be assigned to N-O stretching of NO^+ (Pirngruber & Pieterse, 2006; Gerlach et al., 1999). It was reported that the stretching frequency of NO^+ on HMOR is influenced by an interaction between NO^+ and some other surface species formed on the zeolite (Gerlach et al., 1999). Herein, it should be noticed that although the band at 1698 cm^{-1} for 0.5%Mo/HMOR (spectrum a) was slightly weaker in intensity in comparison with that of HMOR (spectrum b) at 250 °C, it became much stronger than that of HMOR above 300 °C. The relative intensity of the band observed on HMOR and 0.5%Mo/HMOR at different temperatures could be correlated well with the relative activity of the catalysts for C_2H_2-SCR (Fig. 21). Good accordance of NO reduction with the band at 1698 cm^{-1} could also be obtained on NaMOR (Fig 26). The band at 1698 cm^{-1} just appeared at the temperature (spectrum e), where NO conversion to N_2 became significant over the zeolite in C_2H_2-SCR. Based on the above findings, we believe that the species with the band at 1698 cm^{-1} is a crucial intermediate for C_2H_2-SCR over the mordenite-based catalysts.

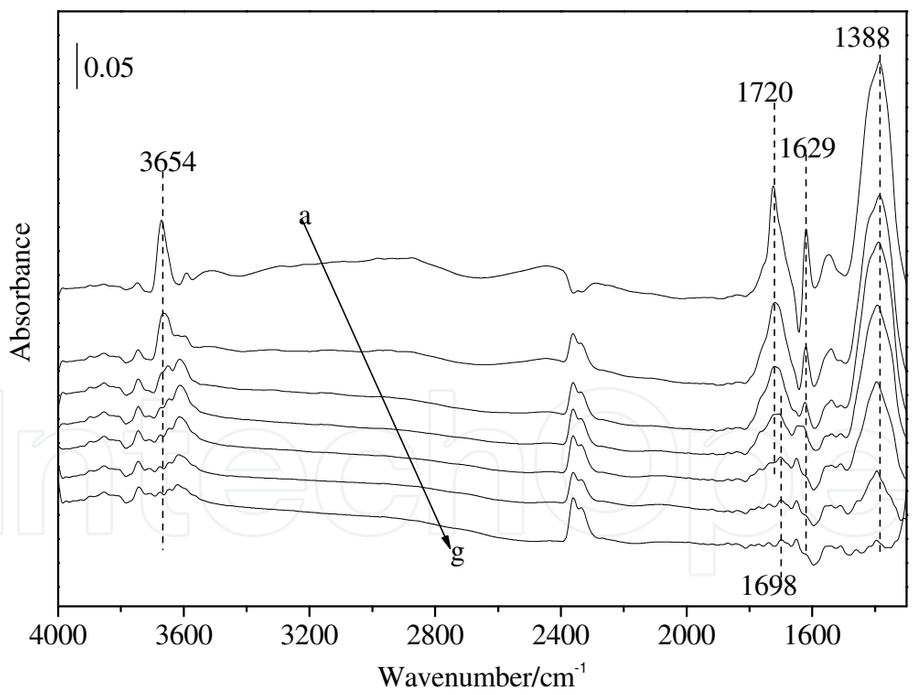

Fig. 26. Steady state in situ FTIR spectra of adsorbed species in gas mixture of 1000 ppm NO + 500 ppm C_2H_2 + 10% O_2 + N_2 on NaMOR at different temperature: 150 °C (a), 200 °C (b), 250 °C (c), 300 °C (d), 350 °C (e), 400 °C (f), 450 °C (g)

To further study the reaction route of C_2H_2-SCR over the catalysts, reactivity of the intermediate (1698 cm^{-1}) was investigated. After a pre-exposure of HMOR to 1000 ppm NO

+ 500 ppm C_2H_2 + 10% O_2/N_2 at 250 ^oC and a followed brief evacuation, the catalyst was exposed to gas mixture of 1000 ppm NO + 10% O_2/N_2. As a result, the intensity of the band at 1698 cm^{-1} rapidly decreased (Fig. 27, spectrum a). It indicates that the intermediate is rather reactive towards $NO+O_2$ at the temperature. On the other hand, no decrease in intensity of the band at 2242 cm^{-1} due to -NCO species could be observed during the period (Fig. 27), indicating that -NCO species is inert towards $NO+O_2$. When the sample was then exposed to gas mixture of 500 ppm C_2H_2 + 10% O_2 in N_2, as shown in Fig. 28 (c~f), the bands both at 2242 cm^{-1} due to -NCO and at 2229 cm^{-1} due to NO^+ disappeared within 1 min. Concomitantly, a band at 1698 cm^{-1} and bands at 3654 and 1629 cm^{-1} due to adsorbed water appeared. It should be noticed that the intensity of the three bands as well as that of the negative band at 3600 cm^{-1} continued to increase within three minutes. The result agrees well with the proposition in literature that isocyanate species can be easily hydrolyzed to amines (Poignant et al., 2001; Bion et al., 2003). Thus, the band at 1698 cm^{-1} can be assigned to acid amide species on the zeolite. It is in accordance with that reported by Poignant et al. (Poignant et al., 2001), who found the species with band at 1694 cm^{-1} in reaction of NO + C_3H_8 + O_2 over HZSM-5 at 350 ^oC.

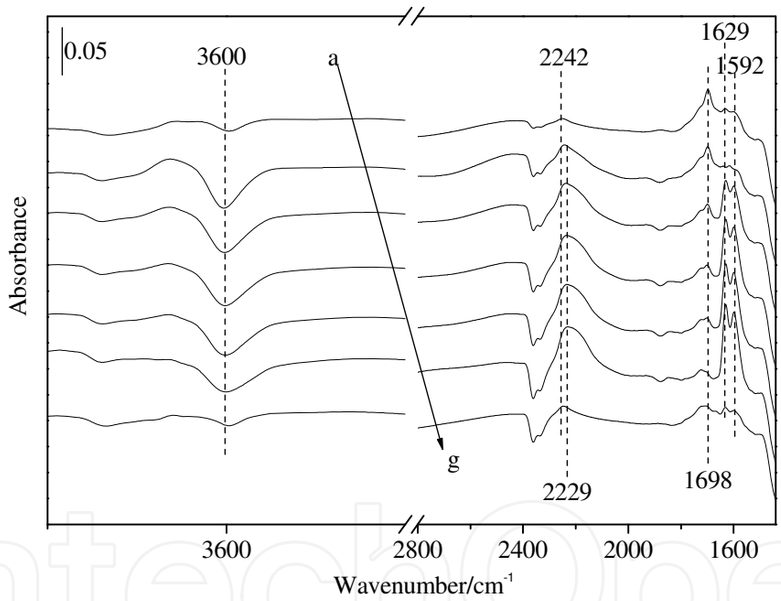

Fig. 27. In situ FTIR spectra of surface species on HMOR at 250 ^oC: a brief evacuation after a pre-exposure of the catalyst to $NO+C_2H_2+O_2$ for 30 min (a), and then when the catalyst was exposed to $NO+O_2$ for: 1 min (b), 3 min (c), 5 min (d), 8 min (e), 30 min (f), and finally evacuated briefly (g)

In Fig. 22, we showed that molybdenum loading on HMOR zeolite considerably promoted the formation of bridging nitrate species. However, neither higher NO conversion to N_2 in C_2H_2-SCR nor stronger band due to the acid amide species (1698 cm^{-1}) could be observed on 0.5%Mo/HMOR compared to HMOR at 250 ^oC. It leads us to speculate that bridging nitrate species (1629 cm^{-1}) may make no contribution to C_2H_2-SCR at the lower temperature (< 250 ^oC) over the mordenite-based catalysts. The speculation was validated by the following experimental results: Although the bridging nitrate species (1629 cm^{-1}) was detected by FTIR

after co-adsorption of $NO+O_2$ on NaMOR at 250 °C (Fig. 22C, spectrum a), no NO conversion to N_2 could be obtained at the temperature (Fig. 21).

Above 300 °C, both C_2H_2-SCR activity (Fig. 21) and the intensity of the band due to acid amide species detected by FTIR (1698 cm^{-1}, in Fig. 25) were larger on 0.5%Mo/HMOR compared to those on HMOR, which corresponds well with the larger population of bridging nitrate species (1629 cm^{-1}, in Fig. 22) given by 0.5%Mo/HMOR in comparison with those given by HMOR at the temperature. The results indicate that bridging nitrate species (1629 cm^{-1}) are also involved in C_2H_2-SCR at higher temperature. Same conclusion can be drawn on NaMOR. The band at 1629 cm^{-1} due to bridging nitrate species arisen from

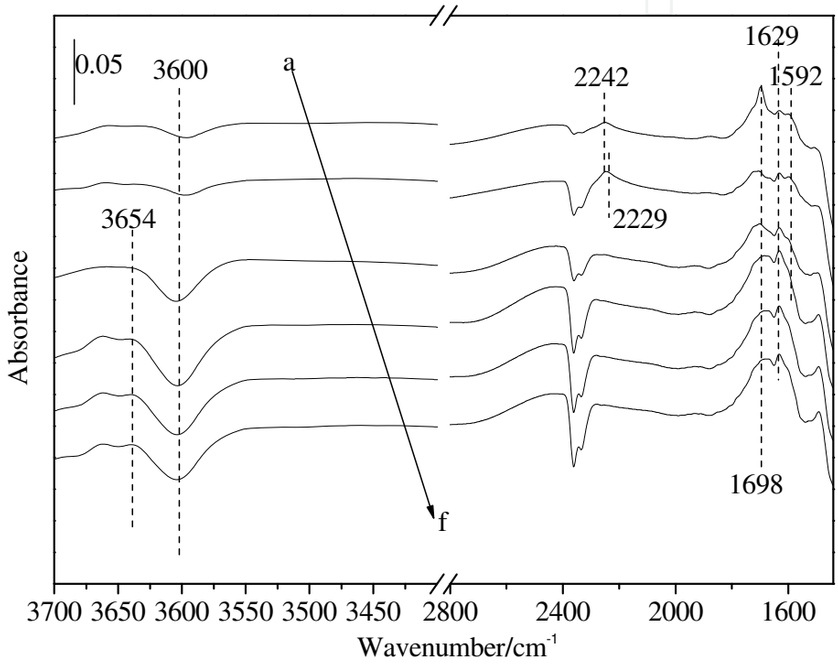

Fig. 28. FTIR spectra of the surface species on HMOR at 250 °C: a brief evacuation after exposing the catalyst to $NO+C_2H_2+O_2$ for 30 min (a), a brief evacuation after exposing the catalyst to $NO+O_2$ for 30 min (b), then exposed the catalyst to $C_2H_2+O_2$ for 1 min (c), 3 min (d), 5 min (e), 30 min (f)

$NO+O_2$ pre-adsorption on the zeolite at 350 °C (Fig. 29, spectrum a) rapidly disappeared when gas mixture of 500 ppm C_2H_2 + 10% O_2/N_2 was introduced to the FTIR cell at this temperature. Correspondingly, band at 1698 cm^{-1} due to acid amide species appeared (Fig. 29, spectrum b). No change of the band at 1388 cm^{-1} in intensity could be observed during this procedure. The results again indicate that bridging nitrate species are involved in the desired reaction at the higher temperature, whereas nitrate species attached to Na^+ have no contribution to C_2H_2-SCR under the reaction condition.

It explains why the C_2H_2-SCR activity of NaMOR became significant when the reaction temperature increased to 350 °C. Thus, the considerably larger activity of 0.5%Mo/HMOR in comparison with that of HMOR for C2H2-SCR above 300 oC (Fig. 21) can be rationally attributed to the larger bridging nitrate formation capacity of the catalyst.

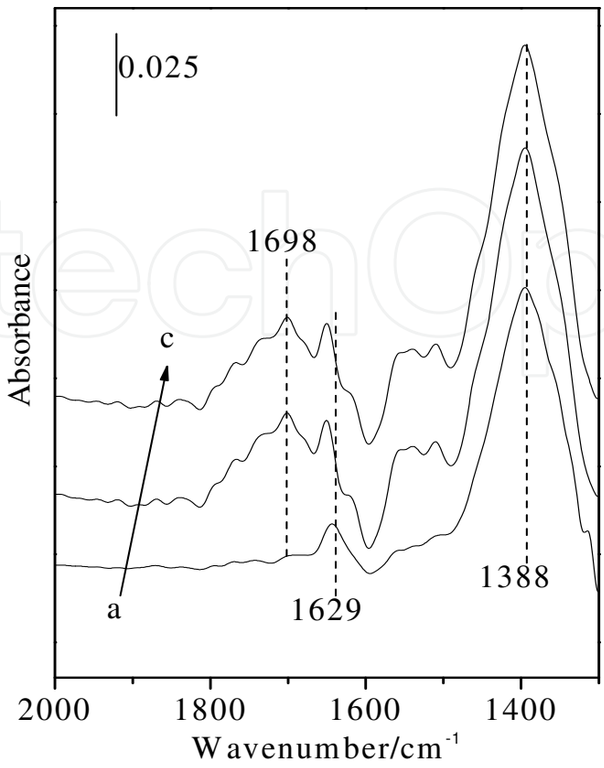

Fig. 29. In situ FTIR spectra of surface species on NaMOR at 350 °C: The catalyst was subjected a brief evacuation after saturation adsorption of 1000 ppm NO and 10 % O_2 in N_2 (a), and then exposed to 500 ppm C_2H_2 + 10 % O_2 / N_2 for 1min (b), 10min (c)

On the basis of above discussion, a possible reaction mechanism of C_2H_2-SCR over the mordenite-based catalysts can be outlined in Scheme 4. Nitrosonium ions (NO^+), bidentate and bridging nitrate species formed by NO+O_2 co-adsorption react first with C_2H_2, leading to isocyanate species (2242 cm^{-1}) formation. The isocyanate species is then rapidly hydrolyzed to the acid amide species (1698 cm^{-1}) that is a crucial intermediate for C_2H_2-SCR over the mordenite-based catalysts.

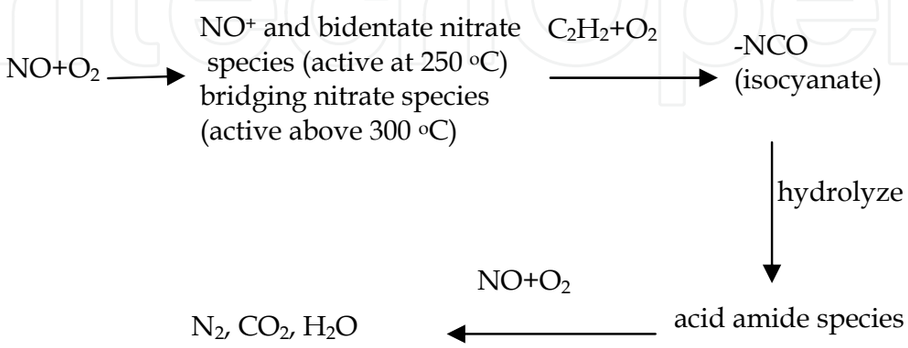

Scheme 4. A possible reaction pathway of the C_2H_2-SCR over the mordenite-based catalysts

As a summarization for C_2H_2-SCR over the mordenite-based catalysts, following reaction mechanism can be drawn: The nitric species, including nitrosonium ions (NO^+) and bidentate nitrate, are fairly active towards the desired reduction in the temperature range of 250-450 ^oC. However, bridging nitrate species begin to make its significant contribution to the reaction above 300 ^oC. Molybdenum incorporated into HMOR zeolite considerably improved the bridging nitrate formation capacity of the catalyst. It explains the promotional effect of molybdenum on C_2H_2-SCR at the higher temperatures. Isocyanate (-NCO), as an active species produced from the reaction of the nitric species with C_2H_2, can be rapidly hydrolyzed to the acid amide species (1698 cm^{-1}) that is a crucial intermediate for C_2H_2-SCR over the mordenite-based catalysts.

5.2 Reaction mechanism of C_2H_2-SCR over Zr/HFER

Surface species formed on 2%Zr/FER by exposing the catalyst to $NO+O_2/N_2$ at 250 ^oC for 30 min and subsequently to C_2H_2/N_2 characterized by FTIR spectra are shown in Fig. 30. NO^+, bridging and bidentate nitrate species, which give the bands at 2188, 1629 and 1598 cm^{-1} (Poignant et al., 2001; Li et al., 2007; Li et al., 2005a; Brosius et al., 2005; Yu et al., 2007) respectively, were presented by the co-adsorption of $NO+O_2$ in N_2 (spectrum a). The three

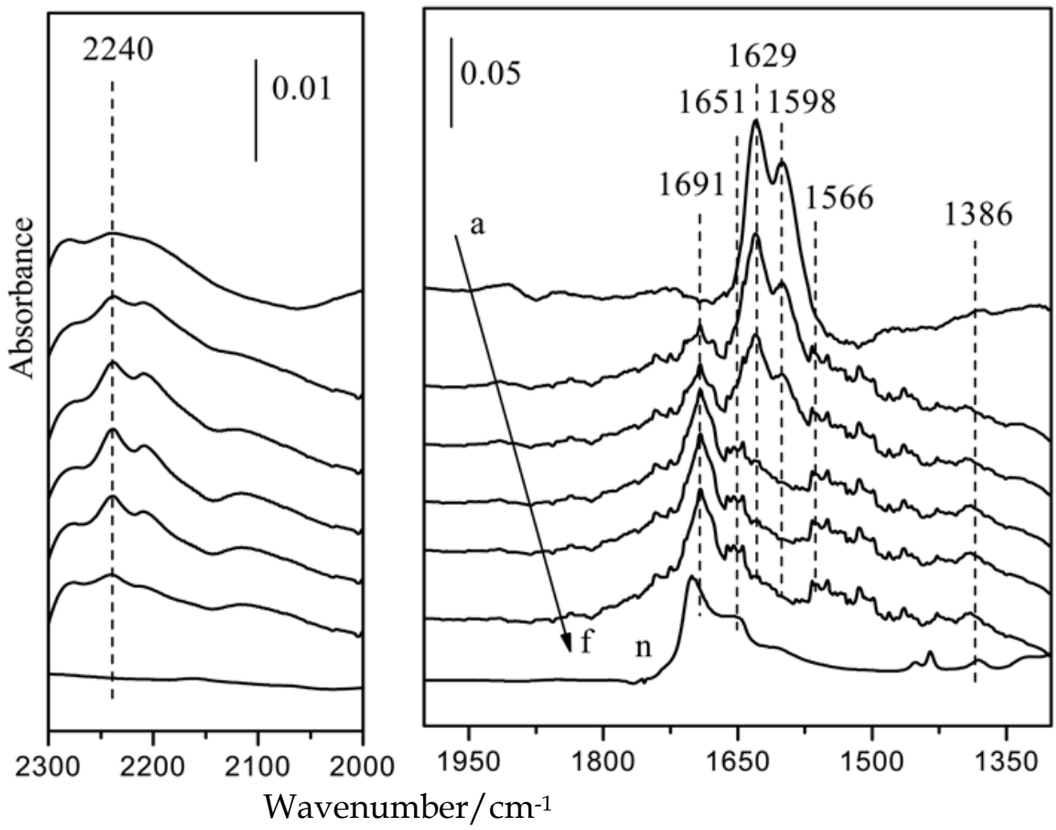

Fig. 30. FTIR spectra of surface species on 2%Zr/FER: the catalyst was exposed to 1000 ppm NO + 10 % O2 + N_2 at 250 ^oC for 30 min (a), and subsequently to 500 ppm C_2H_2 + N_2 for 1 min (b), 2 min (c), 3 min (d), 5 min (e) and 10 min (f); a adsorption steady state got by exposing the fresh catalyst to formamide vapor in N_2 at 150 ^oC (g)

bands rapidly decreased in intensity with an appearance of bands at 2240, 1691, 1651, 1580, 1566 and 1386 cm^{-1} when the gas mixture was switched to $C_2H_2+N_2$. Apparently, the bands at 1651 and 1566 cm^{-1} due to -ONO and $-NO_2$ vibrations [Yeom et al., 2006] increased with time, along with the band at 1691 cm^{-1}. The weak band at 2240 cm^{-1} due to -N=C=O vibration of isocyanate species (Liu et al., 2006) increased in intensity during the first several minutes, and decreased then after, and finally disappeared when the band at 1691 cm^{-1} reached its maximum in intensity. The intensity change of bands at 2240 and 1691 cm^{-1} quite seems that the species giving the band at 1691 cm^{-1} is produced by the isocyanate species.

In literature, Poignant et al. have found the band at 1694 cm^{-1} during the reaction of $NO+C_3H_8+O_2$ over HZSM-5 at 350 ^oC (Poignant et al., 2001) and assigned the band to acetamide species. Larrubia et al. also found a band at 1690 cm^{-1} in FTIR on Fe_2O_3-TiO_2 when they exposed the catalyst to acetamide vapor at 350 ^oC (Larrubia et al., 2001). However, no band at around 1690 cm^{-1}, but at 1717 cm^{-1} was found when we exposed the 2%Zr/HFER catalyst sample to acetamide vapor in N_2 in the temperature range of 30-300 ^oC. Instead, a spectrum that much close to spectrum f (in fig. 30) in shape, with the bands at 1691 and 1386 cm^{-1} along with 1651 cm^{-1} (-ONO vibration) was obtained when the catalyst was exposed to formamide vapor (spectrum g). In addition, the number of carbon in the amine species is also supported by a simultaneously formed formate species with the band at 1580 cm^{-1} (Haneda et al., 2002) (spectra c-f). Hence, we propose that formamide species, which gives the band at 1691 cm^{-1}, was formed during the reaction of C_2H_2-SCR over 2%Zr/FER catalyst by nitric species reacting with acetylene. Correspondingly, a possible formation route of the formamide species can be proposed as follows:

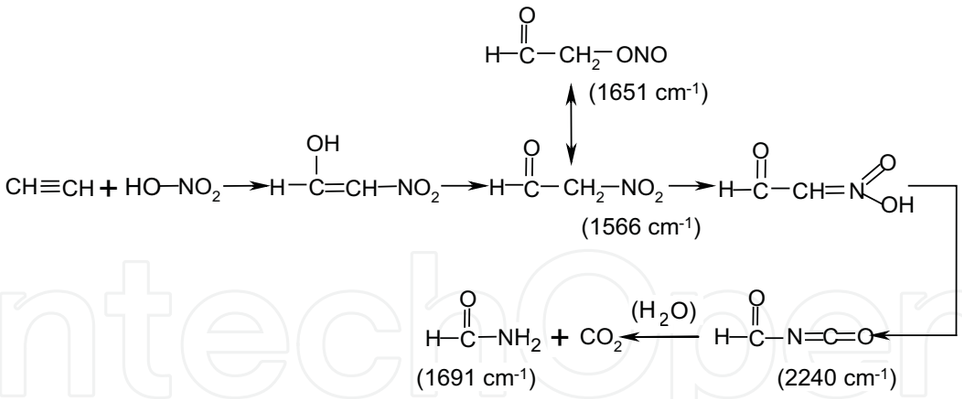

In the reaction of C_2H_2-SCR over 2%Zr/FER, formate species may be produced by the formamide species further reaction with nitric species:

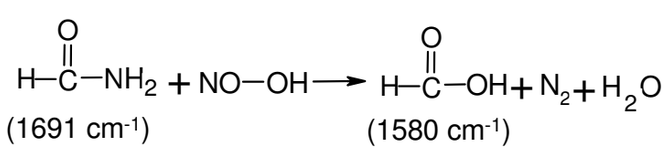

In literature, it is widely accepted that amine species are curtail intermediates of HC-SCR (Poignant et al., 2001; Joubert et al., 2006; Larrubia et al., 2001; Arve et al., 2007). Fig. 31 shows FTIR spectrum of surface species on 2%Zr/FER at 300 ^oC recorded when a

saturated state was reached on the catalyst in the gas mixture of C_2H_2+NO+O_2 in N_2, and the transient spectra recorded when C_2H_2 was cut off from the gas mixture. Obviously, the bands at 1691 cm^{-1} due to formamide species instantly decreased in intensity by switching the gas mixture of C_2H_2+NO+O_2 to NO+O_2, indicating that formamide species is much reactive for reacting with NO+O_2 (and/or nitrate species) over the catalyst at the temperature. The result is in line with the assumption concerning the formate species formation.

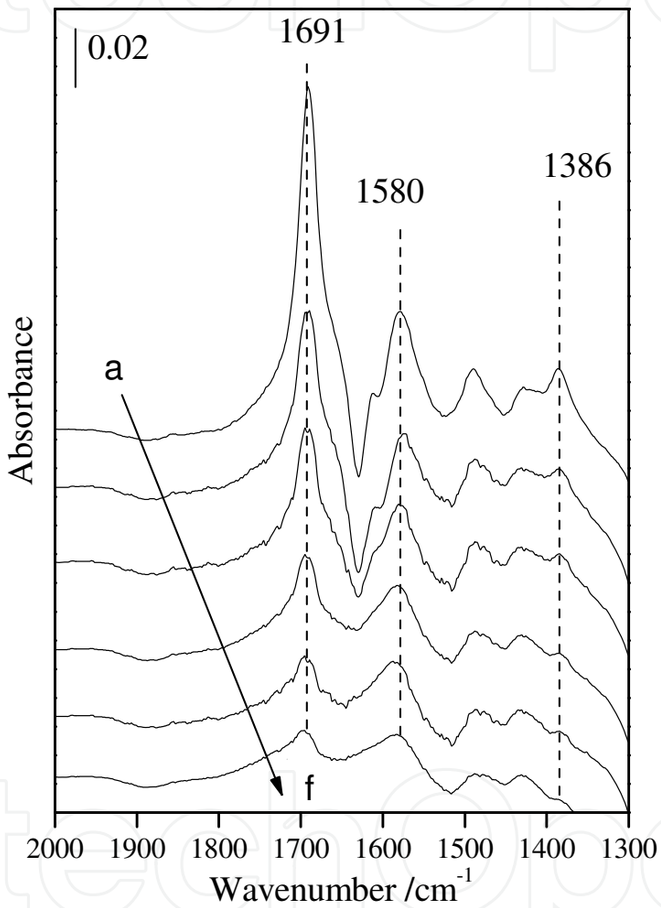

Fig. 31. FTIR spectra of surface species on 2%Zr/FER at 300 ^oC when the catalyst was exposed to 500 ppm C_2H_2 + 1000 ppm NO + 10 % O_2 + N_2 for 25 min (a) and subsequently exposed to 1000 ppm NO + 10 % O_2 + N_2 for 1 min (b), 5 min (c), 10 min (d), 15 min (e) and 30 min (f)

Steady state FTIR spectra of surface species formed on 2%Zr/HFER and HFER in gas mixture of C_2H_2+NO+O_2 in N_2 at some desired temperatures were compared in Fig. 32. The band at 1691 cm^{-1} due to formamide species on 2%Zr/HFER was higher in intensity than that on HFER at each temperature, which may be the result of the higher concentrated nitrate species on 2%Zr/HFER compared to HFER, as discussed in the section 3. It is in good accordance with their order in activity for C_2H_2-SCR (Fig. 8).

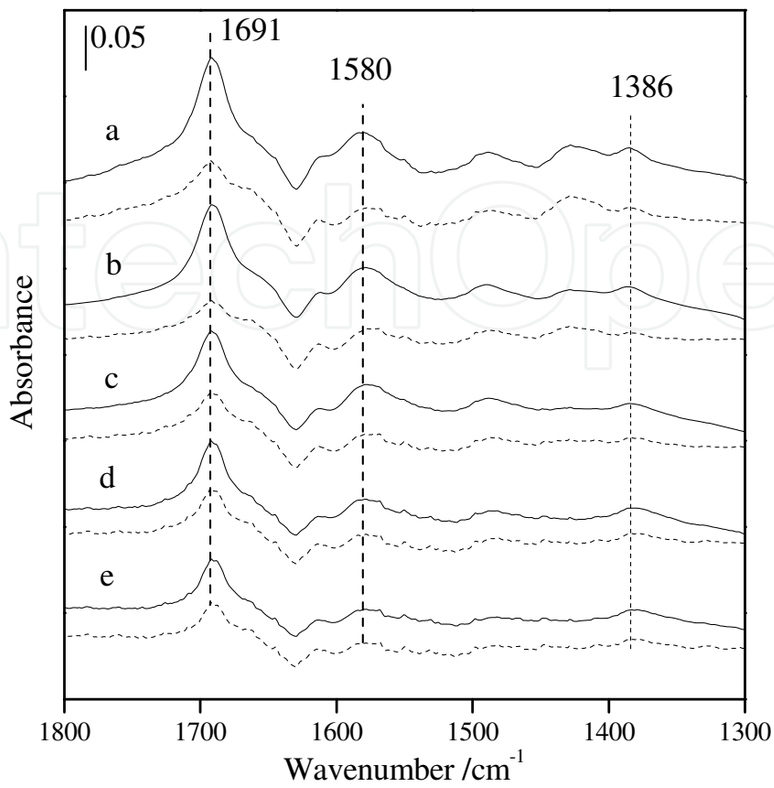

Fig. 32. Steady state in situ FTIR spectra of surface species on 2%Zr/FER (solid curve) and on HFER (dash curve) in gas mixture of 500 ppm C_2H_2 + 1000 ppm NO + 10 % O_2 + N_2 at the temperature: 250 °C (a), 300 °C (b), 350 °C (c), 400 °C (d) and 450 °C

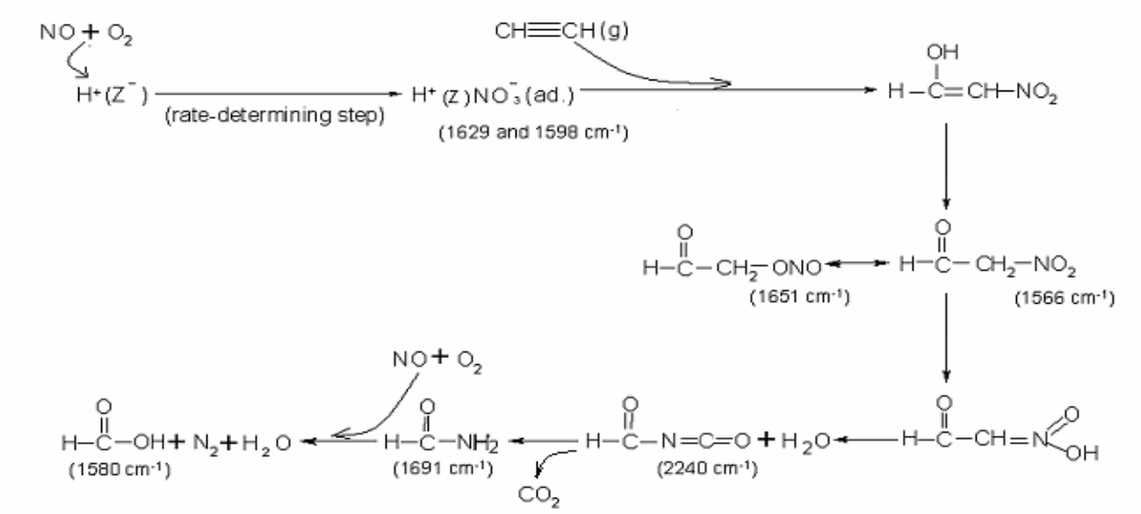

Scheme 5. Possible reaction mechanism of C_2H_2-SCR over Zr/HFER

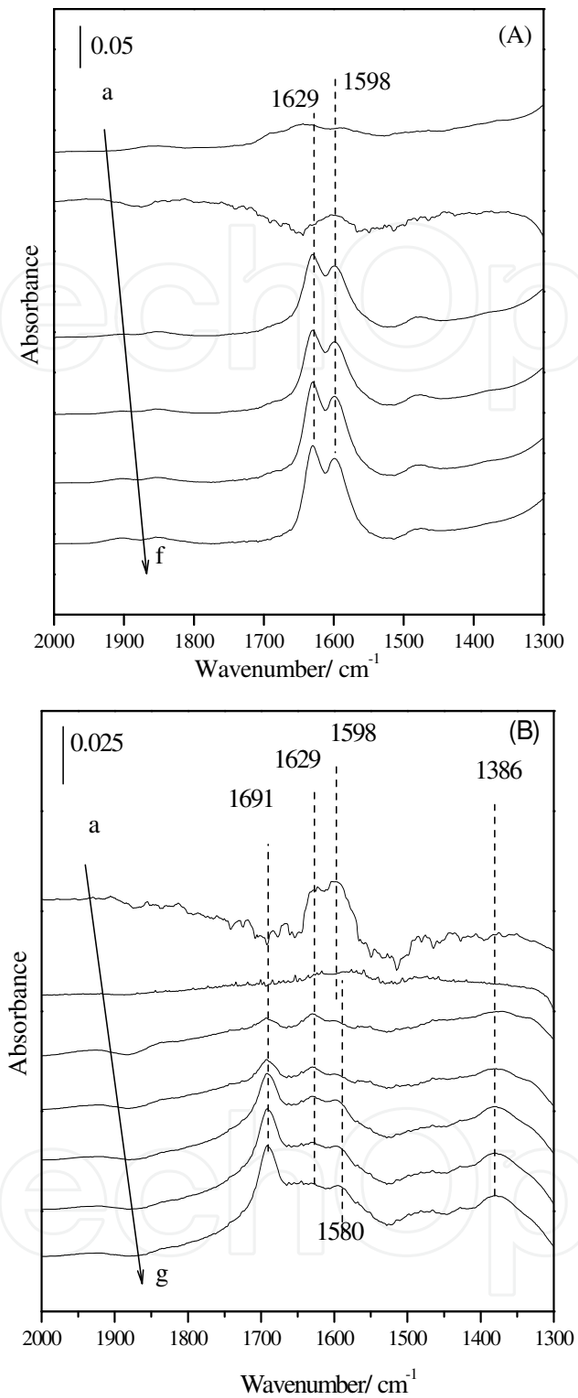

Fig. 33. FTIR spectra of the species recorded on two 2%Zr/FER catalyst wafers at 300 °C: (A) In gas mixture of 500 ppm C_2H_2 + 10 % O_2 + N_2 (a), followed by a brief evacuation (b), then exposed to gas mixture of 1000 ppm NO + 10 % O_2 + N_2 for 1 min (c), 2 min (d), 5 min (e) and 30 min (f). (B) In gas mixture of 1000 ppm NO +10 % O_2 + N_2 (a), followed by a brief evacuation (b), then exposed to gas mixture of 500 ppm C_2H_2 +10 % O_2 + N_2 for 1 min (c), 2 min (d), 5 min (e), 10 min (f) and 30 min (g)

To have an insight into the formation route of formamide species, the reaction of acetylene in gas phase with the species formed on catalyst surface and that between the species were studied in different reaction conditions. No bands due to formamide species could be observed in the following conditions: (1) Gas mixture of C_2H_2+NO+O_2/N_2 was flowed through empty FTIR cell (without catalyst) at 300 ^oC (not shown). (2) Gas mixture of NO+O_2/N_2 was flowed through 2%Zr/HFER at 300 (Fig. 33 A) or 250 ^oC (not shown), before which the catalyst was exposed to C_2H_2+O_2/N_2 for 30 min and evacuated briefly. These results indicate that formamide species can be produced by NO+O_2 reacting neither with C_2H_2 in gas phase nor with the surface species arisen from C_2H_2+O_2 co-adsorption. However, the bands at 1691, 1580 and 1386 cm^{-1} due to formamide and formate species clearly appeared when the catalyst was exposed to gas mixture of C_2H_2+O_2/N_2 at 300 ^oC after a pretreatment in NO+O_2+N_2 for 30 min and briefly evacuated (Fig.33 B). It reveals that formamide species can only be produced by C_2H_2 in gas phase reacting with nitrate species.
Based on above discussion, the reaction mechanism of C_2H_2-SCR over Zr/HFER can be outlined in Scheme 5.

6. The end words of the chapter

For the convenience of reading, we would like to give a note describing the experimental results obtained by FTIR in the chapter to the readers.
The in situ FTIR studies were carried out in a quartz IR cell equipped with CaF_2 windows on a Nicolet 360 FTIR spectrophotometer. All of the spectra were obtained by accumulating 32 scans at a resolution of 2 cm^{-1}. The IR adsorption arising from gas phase on the pathway of infrared laser in the cell were recorded at desired temperature, which was coded as $S_g(T)$. For each experiment, the self-supporting wafer of the catalyst sample was first activated in the cell at 500 ^oC in N_2, and then its IR absorption was measured at each temperature, which was coded as $S_b(T)$. Thus the transient and steady states in situ IR spectra of surface species on the catalyst samples in gas mixtures given in this chapter are those in which the corresponding $S_g(T)$ and $S_b(T)$ were strictly subtracted.

7. Acknowledgments

This corresponding investigation was financially supported by the National Natural Science Foundation of China (Grant No. 20833011 and 20877015) and the State Hi-tech Research and Development Project of the Ministry of Science and Technology of China (Grant No. 2008AA06Z319).

8. References

Anunziata O. A.; Beltramone A. R.; Requejo F. G.. *J. Mol. Catal. A*, 267 (2007) 194.
Arve K.;Backman H.; Klingstedt F.; Eränen K.; Murzin Yu D.. *Appl. Catal. B*, 70 (2007) 65.
Bentrup U.; Brückner A.; Richter M.; Fricke R.. *Appl. Catal. B*, 32 (2001) 229.
Bentrup U.; Richter M.; Fricke R.. *Appl. Catal. B*, 55 (2005) 213.
Berndt H.; Schütze F.-W.; Richter M.; Sowade T.; Grünert W.. *Appl. Catal. B*, 40 (2003) 51
Bion N.; Saussey J.; Haneda M.; Daturi M. *J. Catal*., 217 (2003) 47.
Brosius R.; Bazin P.; Thibault-Starzyk F.; Martens J. A. *J. Catal*., 234 (2005) 191.

Burch R.; Watling T. C.. *Catal. Lett*., 37 (1996) 51.
Chafik T.; Kameoka S.; Ukisu Y.; Miyadera T. *J. Mol. Catal. A*, 136 (1998) 203.
Córdoba L.F.; Fuentes G.A.; Correa C.M.. *Micropor. Mesopor. Mater*., 77 (2005) 193.
Cowan A.D.; Cant N.W.; Haynes B.S.; Nelson P.F. *J. Catal*., 176 (1998) 329.
Delahay G.; Guzmán-Vargas A.; Coq B. *Appl. Catal. B*, 70 (2007) 45.
Dorado F.; de Lucas A.; García P.B.; Romero A.; Valverde J. L. *Ind. Eng. Chem. Res*., 44 (2005) 8988.
Elzey S.; Mubayi A.; Larsen S.C.; Grassian V.H.. *J. Mol. Catal. A*, 285 (2008) 48.
Flores-Moreno J. L.; Delahay G.; Figueras F.; Coq,B.. *J. Catal*., 236 (2005) 292.
Furusawa T.; Seshan K.; Lefferts L.; Aika K.. *Appl. Catal. B*, 39 (2002) 233.
Gerlach T.; Schütze F.W.; Baerns M.. *J. Catal*., 185 (1999) 131.
Goula G.; Katzourakis P.; Vakakis N.; Papadam T.; Konsolakis M. *Catal. Today*, 127 (2007) 199.
Gutierrez L.; Ulla M.A.; Lombardo E.A.; Kovács A.; Lónyi F., Valyon J. *Appl. Catal. A*, 292 (2005) 154.
Gutierrez L.B.; MiróE.E.; Ulla M.A.. *Appl. Catal. A*, 321 (2007) 7.
Hadajiivanov K.; Saussey J.; Freysz J.L.; Lavalley J.C.. *Catal. Lett*., 52 (1998) 103.
Hadjiivanov K.; Penkova A.; Daturi M.; Saussey J.; Lavalley J.C.. *Chem. Phy. Lett*., 377 (2003) 642.
Haneda M.; Bion N.; Daturi M.; Saussey J.; Lavalley J.; Duprez D.; Hamada H. J. *Catal*., 206 (2002) 114.
He C.H.; KÖhler K.. *Phys. Chem. Chem. Phys*., 8 (2006) 898.
He C.H.; Paulus M.; Find J.; Nickl J.A.; Eberle H.J.; Spengler J.. J. *Phys. Chem. B*, 109 (2005) 15906.
He H.; Zhang C.; Yu Y.. *Catal. Today*, 90 (2004) 191.
Held W.; Konig A.; Ritcher T.; Puppe L.. *SAE Paper*, 900496 (1990).
Huuhtanen M.; Kolli T.; Maunula T.; Keiski R.L.. *Catal. Today*, 75 (2002) 379.
Ingelsten H.H.; Zhao D.; Palmqvist A.; Skoglundh M.. J. *Catal*., 232 (2005) 68.
Ivanova E.; Hadjiivanov K.; Klissurski D.; Bevilacqua M.; Armaroli T.; Busca G.. *Micropor. Mesopor. Mater*,46 (2001) 299.
Iwamoto M.; Yahiro H.; Yu-u Y.; Shundo S.; Miauno N.; Shokubai, 32(1990) 430.
Joubert E.; Courtois X.; Marecot P.; Canaff C.; Duprez D.. J. *Catal*., 243 (2006) 252.
Kameoka S.; Ukisu Y.; Miyadera T.. *Phys. Chem. Chem. Phys*., 2 (2000) 367.
Kikuchi E.; Yogo K.. *Catal. Today*, 22 (1994) 73.
Kubacka A.; Janas J.;Włoch E.; Sulikowski B.. *Catal. Today*, 101 (2005) 139.
Kubacka A.; Janas J.; Sulikowski B.. *Appl. Catal. B*, 69 (2006) 43.
Larrubia M. A.; Ramis G.; Busca G.. *Appl. Catal. B*, 30 (2001) 101
Lee T.J.; Nam I.S.; Ham S.W.; Baek Y.S.; Shin K.H.. *Appl. Catal. B*, 41 (2003) 115.
Li G.; Larsen S.C.; Grassian V.H.. *Catal. Lett*., 103 (2005) 23.
Li G.; Larsen S.C.; Grassian V.H.. *J. Mol. Catal. A*, 227 (2005) 25.
Li G..; Wang X.; Jia C.; Liu Z.. *J. Catal*., 257 (2008) 291.
Li L.; Chen J.; Zhang S.; Guan N.; Richter M.; Eckelt R.; Fricke R.. *J. Catal*., 228 (2004) 12
Li L.; Zhang F.; Guan N.; Richter M.; Fricke R.. *Catal. Commun*., 8 (2007) 583.
Li L.; Zhang F.; Guan N.. *Catal. Commun*., 9 (2008) 409.
Li Y.; Armor J.N.. *J. Catal*., 145 (1994) 1.
Liu Z.; Woo S.I.; Lee W.S.. *J. Phys. Chem. B*, 110 (2006) 26019.

Lónyi F.; Valyon J.; GutierreL. Z; Ulla M.A.; Lombardo E.A.. *Appl. Catal. B*, 73 (2007) 1.
Loughran C.E.; Resasco D.E.. *Appl. Catal. B*, 7 (1995) 113.
Luo C.; Li J., Zhu Y.; Hao J.. *Catal. Today*, 119 (2007) 48.
Ma Xiaofei; Wang Xinping; Bi Ran; Zhao Zhen; He Hong. *J. Mol. Catal. A*, 303(2009) 90.
Meunier F.C.; Zuzaniuk V.; Breen J.P.; Olsson M.; Ross J.R.H.. *Catal. Today*, 59 (2000) 287.
Mihaylov M.; Hadjiivanov K.; Panayotov D.; *Appl. Catal. B*, 51 (2004) 33.
Mosqueda-Jiménez B.I.; Jentys A., Seshan K.; Lercher J.A.. *Appl. Catal. B*, 43 (2003) 105.
Mosqueda-Jiménez B.I.; Jentys A.; Seshan K.; Lercher J.A.. *Appl. Catal. B*, 46 (2003) 189.
Nakamoto K.. Infrared Spectra of Inorganic and Coordination Compounds (Mir, Moscow. 1996)
Narbeshuber T.F.; Brait A.; Seshan K.; Lercher J.A.. *J. Catal.*, 172 (1997) 127.
Nishizaka Y.; Misono M.. *Chem. Lett.*, (1994) 2237.
Niu J.; Yang X.; Zhu A.; Shi L.; Sun Q.; Xu Y.; Shi C.. *Catal. Commun*., 7 (2006) 297.
Pieterse J.A.Z.; van den Brink R.W.; Booneveld S.; de Bruijn F.A.. *Appl. Catal. B*, 46 (2003) 239.
Pieterse J.A.Z.; Booneveld S.; *Appl. Catal. B*, 73 (2007) 327.
Pirngruber G.D.; Pieterse J.A.Z.. *J. Catal*., 237 (2006) 237.
Poignant F.; Freysz J.L.; Daturi M.; Sauaaey J.. *Catal. Today*, 70 (2001) 197.
Resini C.; Montanari T.; Nappi L.; Bagnasco G.; Turco M.; Busca G.; Bregani F.. *J. Catal*., 214 (2003) 179.
Sasaki M.; Hamada H.; Kintachi Y.; Ito T.. *Catal. Lett.*, 15 (1992) 297.
Satsuma A.; Yamada K.; Sato K.; Shimizu K.; Hattori T.; Murakami Y.. *Catal. Lett*., 45 (1997) 267.
Satsuma A.; Shimizu K.. *Prog. Ener. Com. Sci*., 29 (2003) 71.
Sedlmair C.; Gil B.; Seshan K.; Jentysa A.; Lercher J.A.. *Phys. Chem. Chem. Phys*., 5 (2003) 1897.
Sedlmair C.; Seshan K.; Jentys A.; Lercher J.A.. *J. Catal*., 214 (2003) 308.
Seijger G.B.F.; van Kooten Niekerk P.; Krishna K.; Calis H.P.A.; van Bekkum H.; van den Bleek C.M.. *Appl. Catal*. B; 40 (2003) 31.
Shi C.; Cheng M.; Qua Z.; Yang X.; Bao X.. *Appl. Catal*. B, 36 (2002) 173.
Shibata J.; Shimizu K.; Satokawa S.; Satsuma A.; Hattori T.. *Phys. Chem. Chem. Phys*., 5 (2003) 2154.
Shibata J.; Takada Y.; Shichi A.; Satokawa S.; Satsuma A.; Hattori T.. *Appl. Catal. B*, 54 (2004) 137.
Shichi A.; Satsuma A.; Iwase M.; Shimizu K.; Komai S.; Hattori T.. *Appl. Catal. B*, 17 (1998) 107.
Shichi A.; Katagi K.; Satsuma A.; Hattori T.. *Appl. Catal. B*, 24 (2000) 97.
Shichi A.; Satsuma A.; Hattori T.. *Appl. Catal. A*, 207 (2001) 315.
Shichi A.; Satsuma A.; Hattori T.. *Appl. Catal. B*, 30 (2001) 25.
Shichi A.; Satsuma A.; Hattori T.. *Catal. Today*, 93–95 (2004) 777.
Shimizu K.; Kawabata H.; Maeshima H.; Satsuma A.; Hattori T.. *J. Phys. Chem. B*, 104 (2000) 2885.
Shimizu K.; Okada F.; Nakamura Y.; Satsuma A.; Hattori T.. *J. Catal*., 195 (2000) 151.
Shimizu K.; Shibata J.; Yoshida H.; Satsuma A.; Hattori T.. *Appl. Catal. B*, 30 (2001) 151.
Shimizu K.; Sugino K.; Kato K.; Yokota S.; Okumura K.; Satsuma A.. *J. Phys. Chem*. C, 111 (2007) 6481.

Stakheev A.Y.; Lee C.W.; Park S.J.; Chong P.J.. *Catal. Lett*., 38 (1996) 271.
Sullivan J. A.; Keane O.. *Appl. Catal*. B, 61 (2005) 244.
Sultana A.; Haneda M.; Fujitani T.; Hamada H.. *Micropor. Mesopor. Mater*., 111 (2008) 488.
Szanyi J.; Paffett M.T.. *J. Catal*., 164 (1996) 232.
Szanyi J.; Kwak J.H.; Moline R.A.; Peden C.H.F.. *Phys. Chem. Chem. Phys*., 5 (2003) 4045.
Szanyi J.; Kwak J.H.; Peden C.H.F.. *J. Phys. Chem. B,* 108 (2004) 3746.
Torre-Abreu C.; Henriques C.; Ribeiro F.R.; Delahay G.; M Ribeiro.F.. *Catal. Today*, 54 (1999) 407.
Tsyntsarski B.; Avreyska V.; Kolev H.; Marinova Ts.; Klissurski D.. J. *Mol. Catal. A*, 193 (2003) 139.
Wang C.; Wang X.; Xing N.; Yu Q.; Wang Y. *Applied Catalysis A*. General 334 (2008) 137.
Wang X.; Xu Y.; Yu S.; Wang C.. *Catal. Lett*., 103 (2005) 101.
Wang X.,; Yu S.; Yang H.; Zhang S..*Appl. Catal. B*, 71 (2007) 246.
Wang X.; Zhang S.; Yu Q.; Yang H.. *Micropor. Mesopor. Mater*., 109 (2007) 298.
Wang X.; Yang H.; Yu Q.; Zhang S.. *Catal. Lett*., 113 (2007) 109.
Wang X.; Yu Q.; Li G.; Liu Z.; *Catal. Lett*., 123 (2008) 289.
Wu Q.; He H.; Yu Y.. *Appl. Catal. B*., 61 (2005) 107.
Xing N.; Wang X., Zhang A.; Liu Z., Guo X.. *Catal. Comm*., 9 (2008) 2117.
X Zhan.; He H.; Ma Z.. *Catal. Comm*., 8 (2007) 187.
Yeom Y. H.; Li M.; Sachtler W. M. H.; Weitz E.. *J.Catal*., 238 (2006) 100.
Yu Q.; Wang X.; Xing N.; Yang H.; Zhang S.. *J. Catal.,* 245 (2007) 124.
Yu Y.; He Hong; Feng Q.; Gao H.; Yang X.. *Appl. Catal*. B, 49 (2004) 159.

IntechOpen

Fourier Transforms - New Analytical Approaches and FTIR Strategies

Edited by Prof. Goran Nikolic

ISBN 978-953-307-232-6
Hard cover, 520 pages
Publisher InTech
Published online 01, April, 2011
Published in print edition April, 2011

New analytical strategies and techniques are necessary to meet requirements of modern technologies and new materials. In this sense, this book provides a thorough review of current analytical approaches, industrial practices, and strategies in Fourier transform application.

How to reference

In order to correctly reference this scholarly work, feel free to copy and paste the following:

Xinping Wang (2011). Fourier Transforms Infrared Spectroscopy Applied in Selective Catalytic Reduction of NO by Acetylene, Fourier Transforms - New Analytical Approaches and FTIR Strategies, Prof. Goran Nikolic (Ed.), ISBN: 978-953-307-232-6, InTech, Available from: http://www.intechopen.com/books/fourier-transforms-new-analytical-approaches-and-ftir-strategies/fourier-transforms-infrared-spectroscopy-applied-in-selective-catalytic-reduction-of-no-by-acetylene

INTECH
open science | open minds

InTech Europe
University Campus STeP Ri
Slavka Krautzeka 83/A
51000 Rijeka, Croatia
Phone: +385 (51) 770 447
Fax: +385 (51) 686 166
www.intechopen.com

InTech China
Unit 405, Office Block, Hotel Equatorial Shanghai
No.65, Yan An Road (West), Shanghai, 200040, China
中国上海市延安西路65号上海国际贵都大饭店办公楼405单元
Phone: +86-21-62489820
Fax: +86-21-62489821

© 2011 The Author(s). Licensee IntechOpen. This chapter is distributed under the terms of the Creative Commons Attribution-NonCommercial-ShareAlike-3.0 License, which permits use, distribution and reproduction for non-commercial purposes, provided the original is properly cited and derivative works building on this content are distributed under the same license.

IntechOpen

IntechOpen